# Supporting Information

# Anisotropy, Segmental Dynamics and Polymorphism of Crystalline Biogenic Carboxylic Acids

*Václav Pokorný[a,b], Petr Touš[a], Vojtěch Štejfa[a], Květoslav Růžička[a], Jan Rohlíček[c], Jiří Czernek[b], Jiří Brus[b], Ctirad Červinka[a,*]*

[a] Department of Physical Chemistry, University of Chemistry and Technology Prague, Technická 5, CZ-166 28 Prague 6, Czech Republic

[b] Institute of Macromolecular Chemistry, Czech Academy of Sciences, Heyrovského nám. 2, CZ-162 06 Prague 6, Czech Republic

[c] Institute of Physics, Czech Academy of Sciences, Na Slovance 2, CZ-182 21 Prague 8, Czech Republic

*Corresponding author: cervinkc@vscht.cz

**This Supporting information contains:**

## Section SI1 Details on the experimental methodology

### SI1.1 Calorimetry

Experimental heat capacities in the ambient region were determined using a Tian-Calvet type calorimeter (SETARAM μDSC IIIa) with a three-step methodology. The measurement of a sample is followed by the measurement of a reference material (synthetic sapphire, NIST Standard reference material No. 720) and by performing a blank experiment. The saturated molar heat capacities $C_{sat}$ obtained in this work are identical to isobaric molar heat capacities $C_{pm}$ in the temperature range studied as (given the very low pressure of the samples) it is not necessary to make a clear distinction between $C_{pm}$ along the saturation curve and $C_{sat}$.

Low-temperature heat capacities were measured using an apparatus Physical Property Measurement System (PPMS) Model 6000 EverCool II (Quantum Design, USA) equipped with a Heat capacity module ($^4$He, $T_{min}$ = 1.8 K). The calorimeter uses thermal-relaxation measurement technique which is alternative to time and labor-intensive adiabatic calorimetry. The specific heat capacity of a sample is determined by the thermal-relaxation method, i. e. from thermal response to a change in heating conditions.[1] Uncertainty of heat capacity obtained using PPMS was investigated recently in our laboratory.[2] The calorimetrically studied samples are listed in Table S1.

To describe temperature dependence of heat capacity in a wide temperature range (from SETARAM μDSC IIIa and Quantum Design PPMS or adiabatic calorimeter), an equation proposed by Archer[3] was used:

$$C_{pm}^{fit} / C_{pm}^{ref} = \left( \frac{T}{T^{ref} f(T) + bT} \right)^3 \quad \text{(SI1)}$$

where $T^{ref}$ = 1 K and $C_{pm}^{ref}$=1 J·K$^{-1}$·mol$^{-1}$ and

$$f(T) = a_i \left(T - T_i\right)^3 + b_i \left(T - T_i\right)^2 + c_i \left(T - T_i\right) + d_i \quad \text{(SI2)}$$

where only a single parameter $d_i$ per each additional temperature interval is to be optimized while the values of the other three are imposed by a constraint of continuity and smoothness of the resulting temperature dependence. Optional parameter *b* is determined from the slope of $f(T)$ at temperatures greater than 70 K.[3]

**Table S1**: Description of the samples subjected to calorimetric investigations.

| Compound | CAS number | Supplier | Sample Preparation | REFCODE | Mole fraction purity |
|---|---|---|---|---|---|
| pyruvic acid | 127-17-3 | Sigma-Aldrich | Molecular sieves | PRUVAC | 0.988[a] |
| citric acid | 77-92-9 | Sigma-Aldrich | Vacuum dried | CITRAC11 | 0.999[a] |
| cis-aconitic acid | 585-84-2 | Sigma-Aldrich | As received | TELZOZ | 0.99[a] |
| α-ketoglutaric acid | 328-50-7 | Sigma-Aldrich | As received | COTPAC | 1.000[a] |
| succinic acid, *β* | 110-15-6 | Sigma-Aldrich | Vacuum dried | SUCACB17 | 0.998[a] |
| succinic acid, *α* | 110-15-6 | - | Annealed at 423 K | SUCACB07 | - |
| fumaric acid, *α* | 110-17-8 | Sigma-Aldrich | Vacuum dried | FUMAAC | 1.000[a] |
| Fumaric acid, *β* | 110-17-8 | - | Annealed at 523 K | FUMAAC01 | - |
| D-malic acid, I | 636-61-3 | Sigma-Aldrich | Vacuum dried | COFRUK11 | 0.983[a] |
| oxaloacetic acid | 328-42-7 | Sigma-Aldrich | Vacuum dried | - | 0.98[a] |

[a] From the certificate of analysis supplied by the manufacturer.

## SI1.2 Solid-state NMR spectroscopy

Solid-state nuclear magnetic resonance (ssNMR) spectra represent fingerprints from which complete crystallographic data can be extracted, often allow to distinguish different polymorphic forms, and to determine the number of symmetry independent molecules in the unit cell. In addition, the NMR crystallography approach has been increasingly utilized to provide a detailed characterization of solid systems. For $^{1}$H and $^{13}$C solid-state NMR of organic molecules, there is a typical maximum discrepancy corresponding to ca. 1% of the chemical shift range, i.e., ca. 0.2 ppm and ca. 2 ppm for $^{1}$H and $^{13}$C, respectively. Larger discrepancies then indicate incorrectly determined structures. When comparing the calculated and experimental resonance frequencies for each atom peak-to-peak, it is then possible to identify the molecular sites, the local geometry of which is distorted from the DFT-optimized model. Such diagnostic deviations reaching up to 1.9 ppm recently found for pyridinium fumarates and their cocrystals opened the questions of lability of these hydrogen-bonded protons, because the NMR experiments usually take place at room temperature, whereas DFT calculations correspond to 0 K.

All ssNMR spectra were measured at 11.7 T using a Bruker AVANCE III HD WB/US NMR spectrometer (Karlsruhe, Germany, 2013) in a double-resonance 4-mm and 3.2-mm probe heads at spinning frequencies $\omega_r/2\pi$ = 10 and 25 kHz, respectively. In all cases, finely powdered, macroscopically dry samples were placed into 4-mm and 3.2-mm $ZrO_2$ rotors. Frictional heating of the rotating samples was compensated for.

**$^{1}$H MAS and $^{13}$C CP/MAS NMR spectroscopy.** $^{1}$H and $^{13}$C magic angle spinning (MAS) and cross-polarization (CP) MAS NMR experiments. The single-pulse $^{1}$H MAS NMR spectra were measured at 25 kHz (MAS frequency). The duration of 90° ($^{1}$H) pulse was 2.3 μs and recycle delay was 30-3000 s depending on the corresponding $T_1$($^{1}$H) relaxation time. The number of scans was eight. The $^{13}$C CP/MAS NMR spectra employing cross-polarization were acquired using the standard pulse scheme at spinning frequency of 10 kHz. The cross-polarization contact time was 1.75 ms. The strength of spin-locking fields $B_1$($^{13}$C) expressed in frequency units $\omega_1/2\pi=\gamma B_1$ was 64 kHz. The spectra were referenced to α-glycine (176.03 ppm). The number of scans was 16-32.

**2D $^{1}$H-$^{1}$H SQ/SQ MAS NMR spectroscopy.** $^{1}$H-$^{1}$H single-quantum/single-quantum (SQ/SQ) spin-diffusion experiment with DUMBO homo-decoupling in both detection periods: the 2D $^{1}$H-$^{1}$H SQ/SQ DUMBO NMR correlation spectra were measured using the NOESY-type pulse sequence with DUMBO homo-decoupling applied in both detection periods (Figure S1). The recycle delay was 30-128 s, $t_1$ evolution period consisted of 128 increments each made of 16-64 scans. The spin-diffusion period (SD) was varied from 20 to 300 μs. The 90° ($^{1}$H) pulse-length was 2.2 μs, power level for DUMBO shape pulse was 71 W, and DUMBO pulse length was 32 μs. All parameters were optimized on glycine to reach maximum spectral resolution ($\Delta\nu(NH^{3+})$=250 Hz and $\Delta\nu(CH_2)$=230 Hz, Figure S1). The $^{1}$H scale was calibrated with external standard – glycine (low-field $NH_3$ signal at 8.5 ppm and the high field α-H signal at 3.0 ppm.

**2D $^{1}$H-$^{1}$H SQ/DQ MAS NMR spectroscopy**: $^{1}$H-$^{1}$H single-quantum/double-quantum (SQ/DQ) correlation experiment with an SPC5 DQ recoupling period and DUMBO homo-decoupling in both detection periods: the 2D $^{1}$H-$^{1}$H DQ/SQ DUMBO NMR correlation spectra were measured using the $^{1}$H-$^{1}$H double-quantum (DQ) experiment employing the SPC5 recoupling sequence at spinning frequency $\omega_r/2\pi$= 10 kHz (Figure S1). The recycle delay was 30−128 s, $t_1$ evolution period consisted of 128 increments each made of 16−64 scans. The DQ coherence excitation and reconversion consisted of 1−4 loops (duration of one loop was 40 μs). The DUMBO decoupling was applied during both detection

periods. Similarly as in the previous case, all the experimental parameters were optimized on glycine sample.

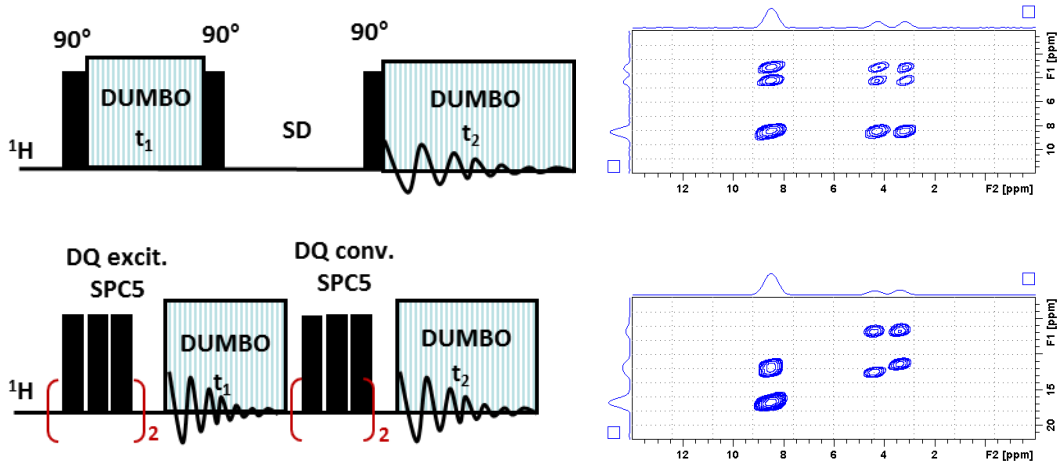


**Figure S1.** Top left - Schematic representation of 2D $^{1}$H-$^{1}$H SQ/SQ DUMBO NMR experiment with a spin-diffusion period; Top right - 2D $^{1}$H-$^{1}$H SQ/SQ DUMBO NMR spectrum (10 kHz) of glycine measured with a 500 μs mixing period; Bottom left - Schematic representation of 2D $^{1}$H-$^{1}$H DQ/SQ DUMBO NMR experiment with SPC5 recoupling sequence; Bottom right - 2D $^{1}$H-$^{1}$H DQ/SQ DUMBO spectrum (10 kHz) of glycine measured with a 80 μs recoupling period.

## Section SI2 Detailed results on the crystal structures

### SI2.1 X-ray diffraction results

The collected variable-temperature XRPD patterns are given in Figure S2 and the derived unit cell parameters are given in Table S2. Apart from succinic acid and few other random data points, there have been often only single crystal structure entries in the literature for these carboxylic acids (pyruvic,[4] citric,[5] α-ketoglutaric,[6] fumaric,[7] succinic,[8-13] malic[14]) collected at ambient temperature. Such molar volumes differ from the experimental results collected in this work by 0.1%, indicating a good mutual data consistency. This deviation amounts to 0.4% for succinic acid, which is given by a relatively larger scatter of the literature data.

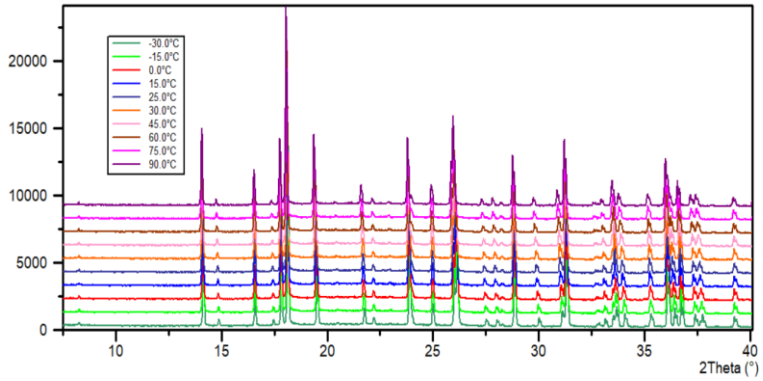


Citric acid

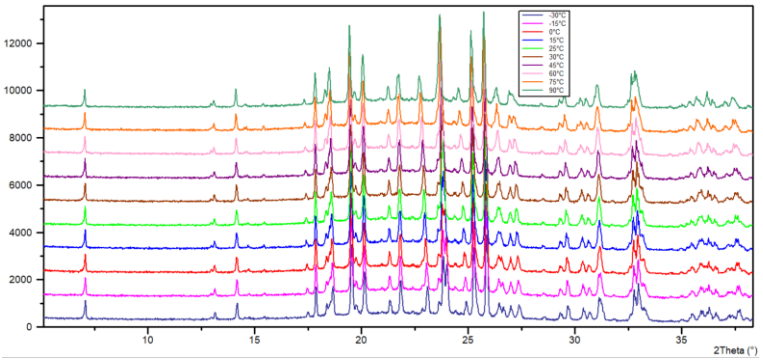


*cis*-Aconitic acid

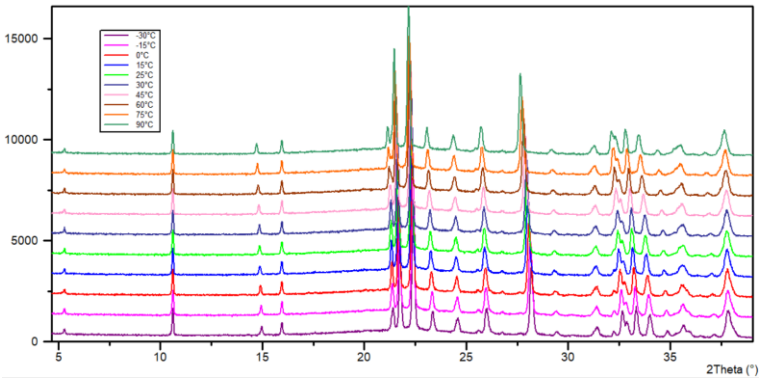


α-Ketoglutaricic acid

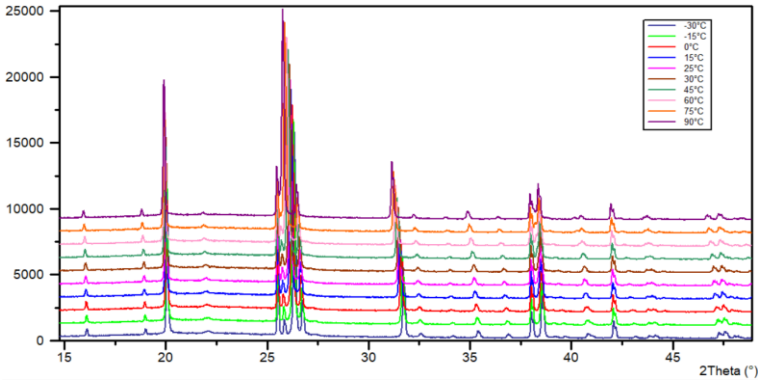


Succinic acid

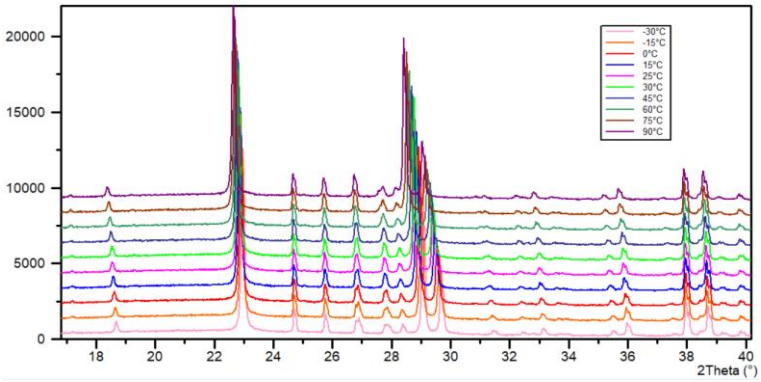


Fumaric acid

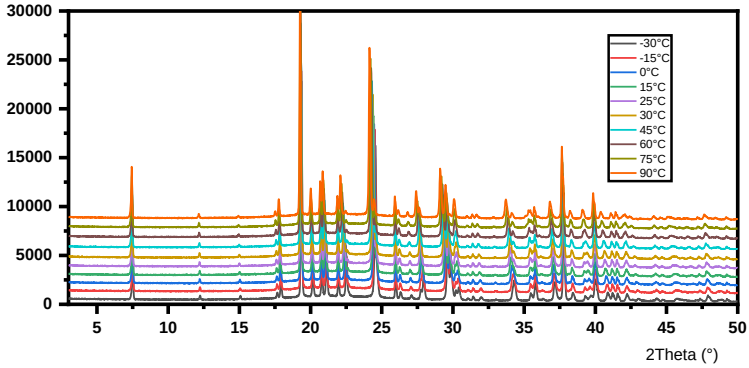


L-Malic acid

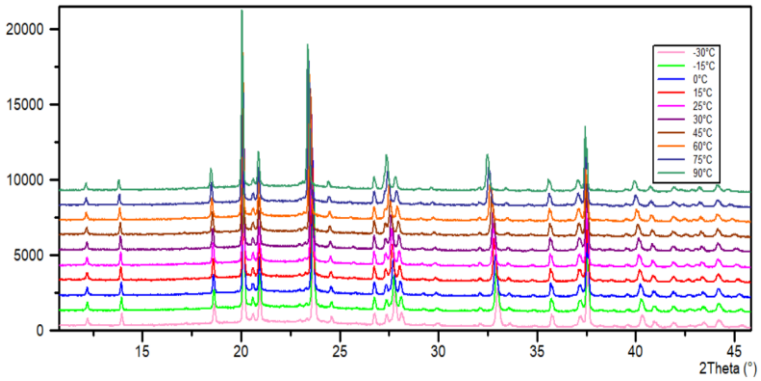


DL-Malic acid

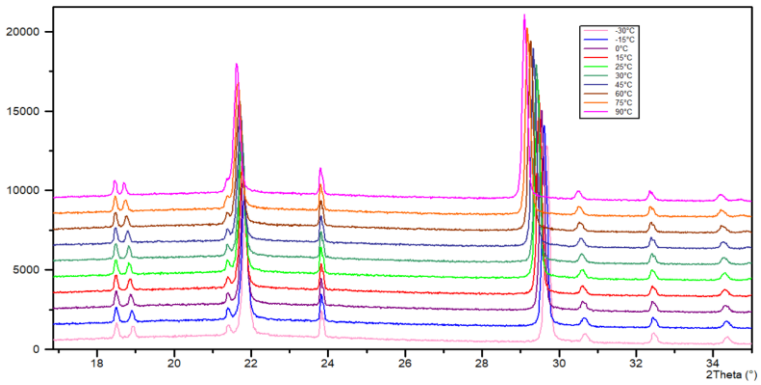


**Figure S2.** Variable-temperature XRPD patterns collected in the temperature range from −30 °C to 90 °C with a step 15 °C.

**Table S2**: Experimental unit-cell parameters (*a*, *b*, *c* in Å; angles in deg.) determined with variable temperature X-ray diffraction.

| *T*, K | *a* | *b* | *c* | *β* |
|---|---|---|---|---|
| | | Citric acid | | |
| 243.15 | 12.7700 ± 0.0002 | 5.6093 ± 0.0001 | 11.4630 ± 0.0001 | 111.3300 ± 0.0007 |
| 258.15 | 12.7830 ± 0.0001 | 5.6129 ± 0.0001 | 11.4640 ± 0.0001 | 111.3000 ± 0.0006 |
| 273.15 | 12.7950 ± 0.0002 | 5.6166 ± 0.0001 | 11.4650 ± 0.0001 | 111.2700 ± 0.0007 |
| 288.15 | 12.8070 ± 0.0002 | 5.6205 ± 0.0001 | 11.4670 ± 0.0001 | 111.2500 ± 0.0007 |
| 303.15 | 12.8190 ± 0.0002 | 5.6244 ± 0.0001 | 11.4690 ± 0.0001 | 111.2200 ± 0.0008 |
| 318.15 | 12.8310 ± 0.0002 | 5.6285 ± 0.0001 | 11.4710 ± 0.0001 | 111.1900 ± 0.0008 |
| 333.15 | 12.8420 ± 0.0002 | 5.6331 ± 0.0001 | 11.4730 ± 0.0001 | 111.1500 ± 0.0007 |
| 348.15 | 12.8540 ± 0.0002 | 5.6375 ± 0.0001 | 11.4760 ± 0.0001 | 111.1300 ± 0.0006 |
| 363.15 | 12.8650 ± 0.0001 | 5.6422 ± 0.0001 | 11.4790 ± 0.0001 | 111.0900 ± 0.0006 |
| | | *α*-Ketoglutaric acid | | |
| 243.15 | 16.7020 ± 0.0006 | 6.3250 ± 0.0002 | 5.5047 ± 0.0003 | 94.7340 ± 0.0026 |
| 258.15 | 16.7030 ± 0.0006 | 6.3376 ± 0.0002 | 5.5105 ± 0.0003 | 94.7600 ± 0.0027 |
| 273.15 | 16.7040 ± 0.0007 | 6.3509 ± 0.0002 | 5.5156 ± 0.0003 | 94.7870 ± 0.0028 |
| 288.15 | 16.7060 ± 0.0007 | 6.3646 ± 0.0002 | 5.5213 ± 0.0003 | 94.8140 ± 0.0027 |
| 303.15 | 16.7080 ± 0.0007 | 6.3791 ± 0.0002 | 5.5268 ± 0.0003 | 94.8380 ± 0.0028 |
| 318.15 | 16.7100 ± 0.0007 | 6.3947 ± 0.0002 | 5.5328 ± 0.0003 | 94.8670 ± 0.0028 |
| 333.15 | 16.7110 ± 0.0007 | 6.4112 ± 0.0002 | 5.5392 ± 0.0003 | 94.9090 ± 0.0028 |
| 348.15 | 16.7110 ± 0.0007 | 6.4285 ± 0.0002 | 5.5450 ± 0.0003 | 94.9550 ± 0.0029 |
| 363.15 | 16.7130 ± 0.0008 | 6.4473 ± 0.0002 | 5.5513 ± 0.0003 | 95.0200 ± 0.0030 |
| | | Succinic acid | | |
| 243.15 | 5.4996 ± 0.0002 | 8.8393 ± 0.0002 | 5.0700 ± 0.0002 | 92.0850 ± 0.0013 |
| 258.15 | 5.5045 ± 0.0002 | 8.8488 ± 0.0002 | 5.0771 ± 0.0002 | 91.9540 ± 0.0014 |
| 273.15 | 5.5097 ± 0.0002 | 8.8584 ± 0.0002 | 5.0844 ± 0.0001 | 91.8160 ± 0.0013 |
| 288.15 | 5.5152 ± 0.0002 | 8.8680 ± 0.0002 | 5.0922 ± 0.0001 | 91.6710 ± 0.0014 |
| 303.15 | 5.5214 ± 0.0002 | 8.8774 ± 0.0002 | 5.1003 ± 0.0001 | 91.5190 ± 0.0014 |
| 318.15 | 5.5283 ± 0.0002 | 8.8866 ± 0.0002 | 5.1091 ± 0.0001 | 91.3500 ± 0.0015 |
| 333.15 | 5.5360 ± 0.0002 | 8.8960 ± 0.0002 | 5.1189 ± 0.0001 | 91.1650 ± 0.0015 |
| 348.15 | 5.5447 ± 0.0002 | 8.9047 ± 0.0002 | 5.1291 ± 0.0002 | 90.9660 ± 0.0016 |
| 363.15 | 5.5551 ± 0.0002 | 8.9127 ± 0.0002 | 5.1405 ± 0.0002 | 90.7360 ± 0.0017 |
| | | Fumaric acid | | |
| 243.15 | 7.6145 ± 0.0001 | 14.9600 ± 0.0003 | 6.5835 ± 0.0001 | 111.150 ± 0.0024 |

| | | | | |
|---|---|---|---|---|
| 258.15 | 7.6141 ± 0.0001 | 14.9730 ± 0.0003 | 6.5980 ± 0.0001 | 111.120 ± 0.0024 |
| 273.15 | 7.6138 ± 0.0001 | 14.9870 ± 0.0003 | 6.6128 ± 0.0001 | 111.080 ± 0.0024 |
| 288.15 | 7.6135 ± 0.0001 | 15.0020 ± 0.0003 | 6.6279 ± 0.0001 | 111.050 ± 0.0025 |
| 303.15 | 7.6132 ± 0.0001 | 15.0170 ± 0.0003 | 6.6434 ± 0.0001 | 111.010 ± 0.0025 |
| 318.15 | 7.6131 ± 0.0002 | 15.0330 ± 0.0003 | 6.6600 ± 0.0001 | 110.980 ± 0.0026 |
| 333.15 | 7.6129 ± 0.0002 | 15.0480 ± 0.0004 | 6.6774 ± 0.0001 | 110.930 ± 0.0028 |
| 348.15 | 7.6127 ± 0.0002 | 15.0640 ± 0.0004 | 6.6955 ± 0.0002 | 110.900 ± 0.0030 |
| 363.15 | 7.6128 ± 0.0002 | 15.0810 ± 0.0004 | 6.7146 ± 0.0001 | 110.850 ± 0.0028 |
| | | L- Malic acid | | |
| 243.15 | 5.0289 ± 0.0001 | 9.1635 ± 0.0002 | 11.7750 ± 0.0003 | 93.7890 ± 0.0010 |
| 258.15 | 5.0340 ± 0.0001 | 9.1686 ± 0.0002 | 11.7900 ± 0.0003 | 93.8940 ± 0.0010 |
| 273.15 | 5.0390 ± 0.0001 | 9.1737 ± 0.0002 | 11.8060 ± 0.0003 | 94.0060 ± 0.0010 |
| 288.15 | 5.0444 ± 0.0001 | 9.1788 ± 0.0002 | 11.8220 ± 0.0003 | 94.1190 ± 0.0010 |
| 303.15 | 5.0500 ± 0.0001 | 9.1848 ± 0.0002 | 11.8390 ± 0.0003 | 94.2350 ± 0.0010 |
| 318.15 | 5.0558 ± 0.0001 | 9.1903 ± 0.0002 | 11.8550 ± 0.0003 | 94.3640 ± 0.0012 |
| 333.15 | 5.0627 ± 0.0001 | 9.1968 ± 0.0002 | 11.8740 ± 0.0003 | 94.4970 ± 0.0011 |
| 348.15 | 5.0698 ± 0.0001 | 9.2030 ± 0.0002 | 11.8930 ± 0.0003 | 94.6350 ± 0.0010 |
| 363.15 | 5.0780 ± 0.0001 | 9.2094 ± 0.0002 | 11.9120 ± 0.0003 | 94.7860 ± 0.0010 |
| | | DL- Malic acid | | |
| 243.15 | 4.8877 ± 0.0001 | 8.8130 ± 0.0001 | 13.0280 ± 0.0002 | 103.280 ± 0.0017 |
| 258.15 | 4.8901 ± 0.0001 | 8.8173 ± 0.0001 | 13.0380 ± 0.0002 | 103.180 ± 0.0016 |
| 273.15 | 4.8927 ± 0.0001 | 8.8219 ± 0.0001 | 13.0490 ± 0.0002 | 103.070 ± 0.0016 |
| 288.15 | 4.8959 ± 0.0001 | 8.8266 ± 0.0001 | 13.0590 ± 0.0002 | 102.970 ± 0.0016 |
| 303.15 | 4.8992 ± 0.0001 | 8.8313 ± 0.0001 | 13.0700 ± 0.0002 | 102.870 ± 0.0015 |
| 318.15 | 4.9028 ± 0.0001 | 8.8362 ± 0.0001 | 13.0800 ± 0.0002 | 102.760 ± 0.0015 |
| 333.15 | 4.9064 ± 0.0001 | 8.8414 ± 0.0001 | 13.0940 ± 0.0002 | 102.620 ± 0.0015 |
| 348.15 | 4.9097 ± 0.0001 | 8.8464 ± 0.0001 | 13.1070 ± 0.0002 | 102.480 ± 0.0015 |
| 363.15 | 4.9133 ± 0.0001 | 8.8522 ± 0.0001 | 13.1220 ± 0.0002 | 102.320 ± 0.0016 |
| | | Oxaloacetic acid | | |
| 243.15 | 8.6831 ± 0.0004 | 6.0153 ± 0.0003 | 5.5746 ± 0.0003 | 120.7700 ± 0.0028 |
| 258.15 | 8.6846 ± 0.0004 | 6.0283 ± 0.0003 | 5.5764 ± 0.0003 | 120.7800 ± 0.0028 |
| 273.15 | 8.6862 ± 0.0004 | 6.0416 ± 0.0003 | 5.5784 ± 0.0004 | 120.7900 ± 0.0028 |
| 288.15 | 8.6880 ± 0.0004 | 6.0558 ± 0.0003 | 5.5807 ± 0.0004 | 120.8000 ± 0.0029 |
| 303.15 | 8.6884 ± 0.0004 | 6.0652 ± 0.0003 | 5.5819 ± 0.0004 | 120.7900 ± 0.0030 |
| 318.15 | 8.6887 ± 0.0004 | 6.0693 ± 0.0003 | 5.5820 ± 0.0003 | 120.8000 ± 0.0029 |
| 333.15 | 8.6904 ± 0.0004 | 6.0839 ± 0.0003 | 5.5838 ± 0.0003 | 120.8100 ± 0.0030 |
| 348.15 | 8.6924 ± 0.0005 | 6.0997 ± 0.0003 | 5.5861 ± 0.0004 | 120.8200 ± 0.0030 |
| 363.15 | 8.6931 ± 0.0005 | 6.1154 ± 0.0003 | 5.5882 ± 0.0004 | 120.8200 ± 0.0030 |

## SI2.2 Structure solution of crystalline oxaloacetic acid form XRPD data

An extra XRPD experiment was performed to obtain a high-quality powder diffraction data suitable for the crystal structure determination process. The XRPD data were measured at room temperature from 4° to 100° 2$\theta$ with 0.013° step size and with an overall measurement time of 66 hours. The indexing in the program DICVOL06[15] found a monoclinic unit cell with a reasonable high figure of merit $F(N)$ = 36. However, this unit cell does not explain several weak peaks in the pattern. The consequent indexing in other software (CRYSFIRE 2020 and Conograph[16]) did not find any other reasonable unit cell and we concluded that the additional observed peaks in the pattern are most probably due to the small amount

of the impurity phase or due to the modulation. The Le Bail fitting in Jana2020[17] revealed significant anisotropic broadening of diffraction peaks in the pattern. Anisotropic strain broadening tensor had thus to be introduced and its parameters were refined to model the anisotropy in the peak broadening.
The crystal structure determination was done in the program Superflip[18] with combination of manual atomic placement in the program MCE[19] The most probable space group is Cm with a molecule lying on a mirror symmetry. The Rietveld refinement in Jana2020, depicted in Figure S3, showed that restraints for bond and bond angles had to be introduced to keep the model in a reasonable molecular geometry. Unfortunately, this led to the fact, that the powder diffraction cannot distinguish between possible enol or keto form of the molecule. Four possible models of restraints were created, combining the enol or keto molecular form and two possible combinations of the position of the hydrogen atom in the carboxyl groups. After the refinement, all these four possible combinations had comparable *R* values and we were not able to distinguish the correct form. However, the closer inspection of the final bond distances revealed, that in cases of keto forms, the model did not strictly follow the restraints. The double bonds were elongated, and on the other hand, the single bonds are shorter, than expected. This observation indicates that the molecule most likely exists in its enol form. The clear insight into this problem was only given by the results of ssNMR that confirmed the presence of the enol form. The final structure solution was uploaded to the CSD database with the Deposition Number 2183126.

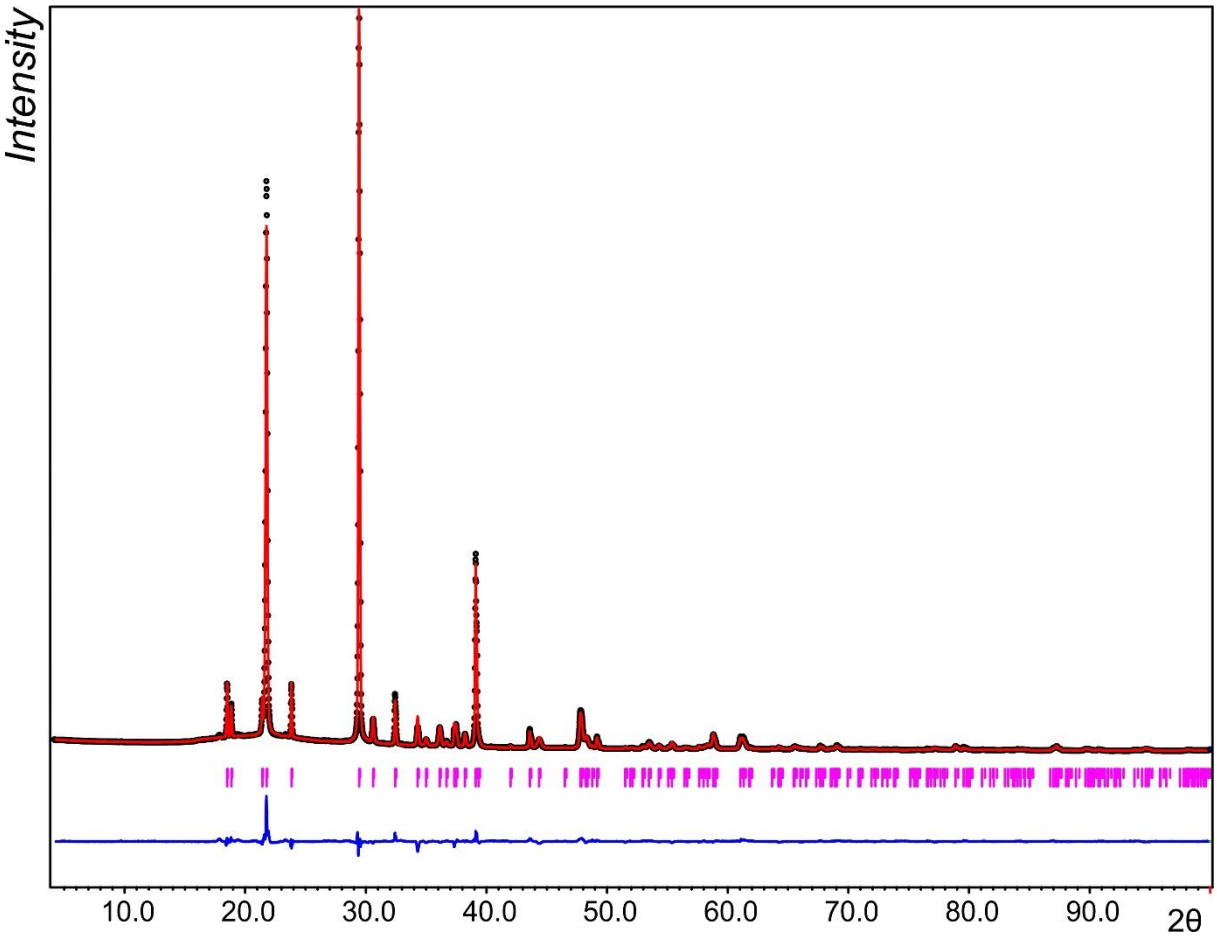


**Figure S3.** The final Rietveld fit of the XRPD pattern of the oxaloacetic acid. The black dots – measured XRPD pattern, red line – calculated XRPD pattern, blue line – difference curve and magenta vertical bars shows Bragg's positions.

## SI2.3 Controlled extrapolation of X-ray diffraction results

Since variable-temperature crystal structure measurements for molecular crystals are rather rare, we tested three extrapolation schemes exploiting our X-ray structures collected at nearly-ambient temperatures, and optionally our PBE-D3/PAW results, to extrapolate the crystal volumes down to the absolute zero. Comparison of these extrapolations with the low-temperature literature structures can be sufficiently performed only for succinic acid, as illustrated in Figure S4. We conclude that it is most accurate to use the following three-step procedure: i) to derive the thermal expansivity as a function of temperature from the calculated volumes; ii) to scale it with a linear function so that the scaled expansivity reproduces the one derived from the experimental data at nearly ambient temperatures; iii) to gradually extrapolate the experimental volumes using the scaled thermal expansivity, being a linear function of temperature, constrained to zero value at the absolute zero. Alternative approaches, using only extrapolations of the experimental volumes, or scaling of the calculated volumes instead of the expansivities yielded imperfect volume trends, exhibiting exaggerated slopes or too large expansivity in the vicinity of the absolute zero, as depicted in Figure S4.

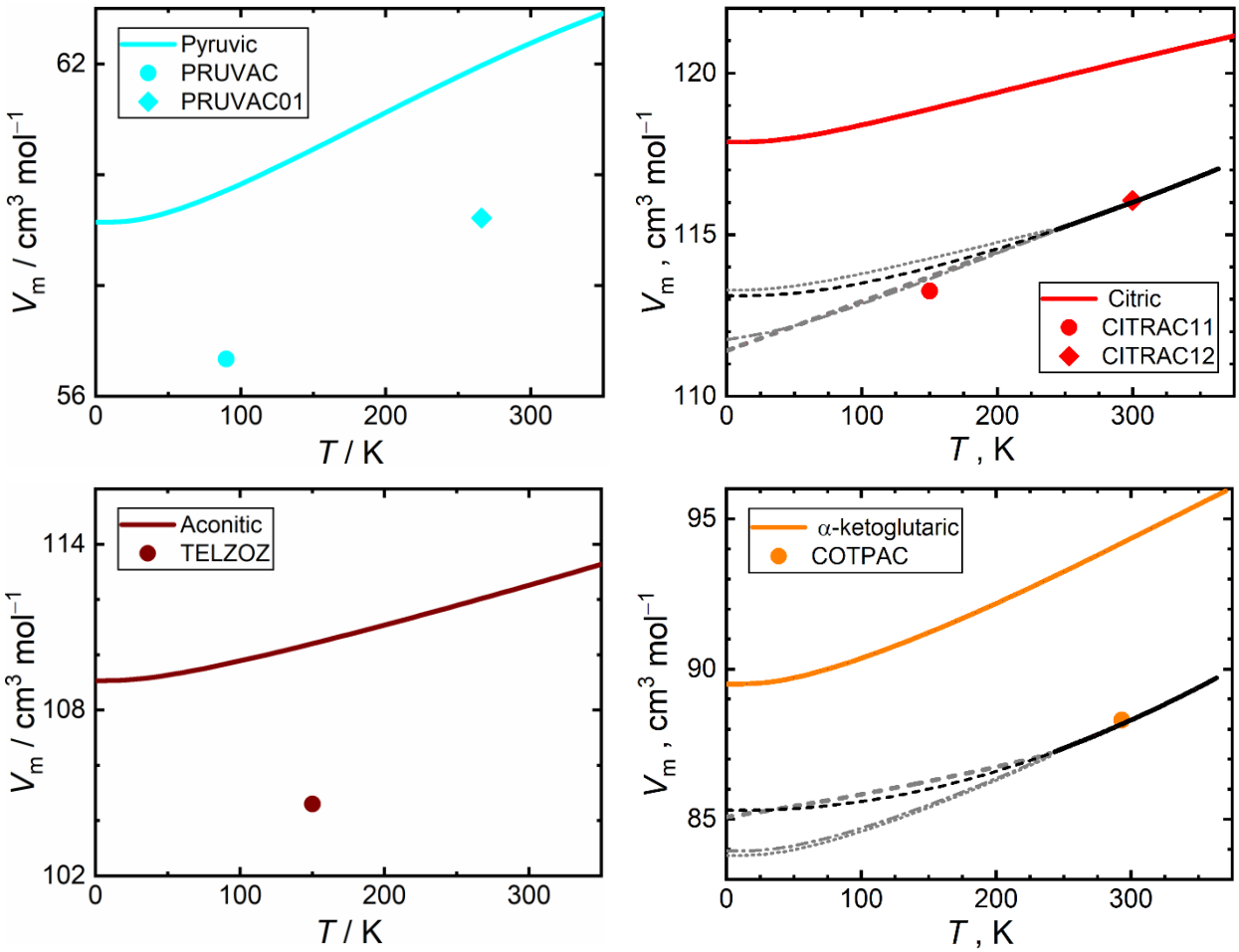

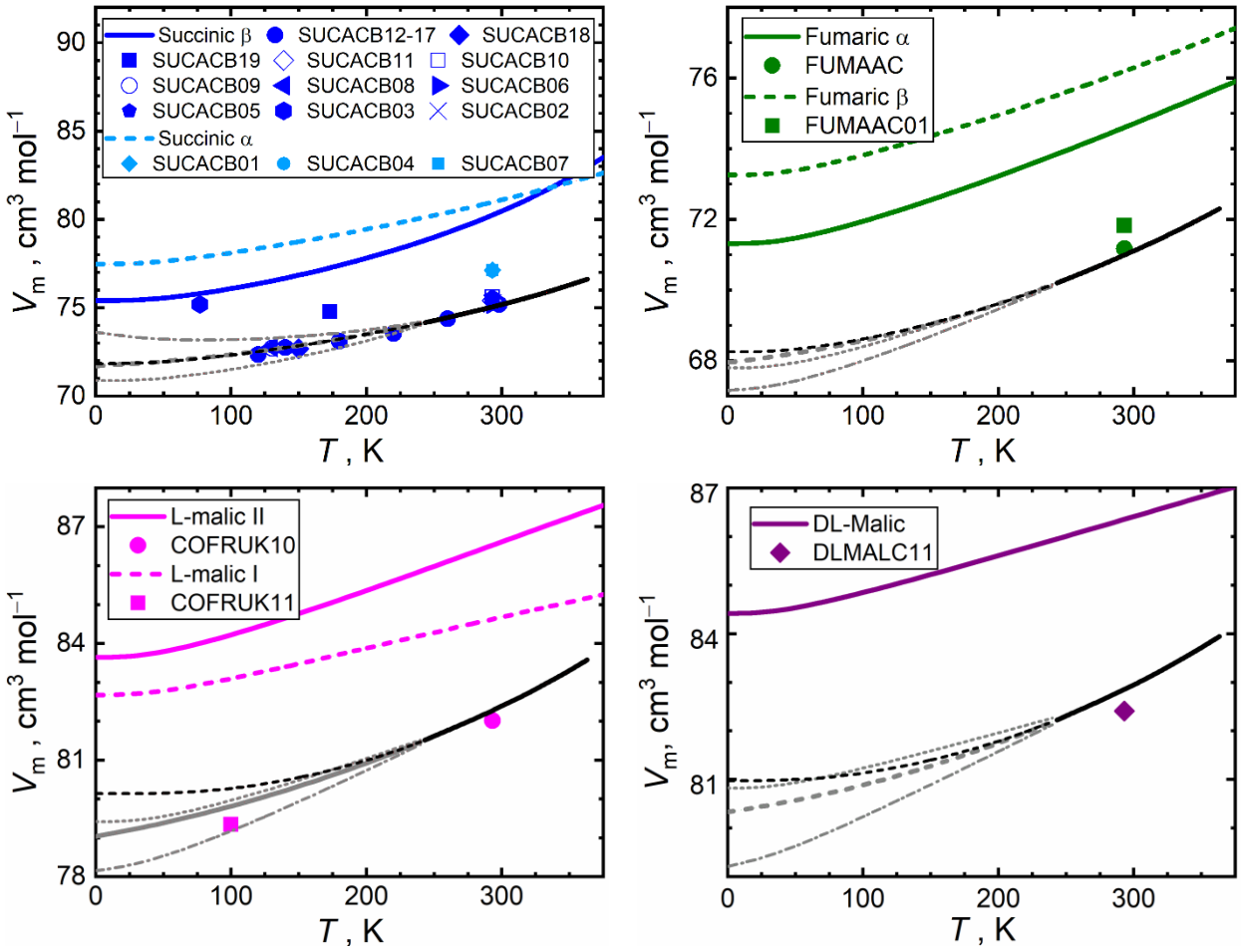


**Figure S4.** Overview of quasi-harmonic molar volumes (colored lines) and their experimental counterparts culled from the following references. Pyruvic acid: ♦ – PRUVAC,[4] ● – PRUVAC01[20]; Citric acid: ● – CITRAC11,[21] ♦ – CITRAC12[5]; Aconitic acid: ● – TELZOZ[22]; Ketoglutaric acid: COTPAC[6]; Succinic acid: × – SUCACB02,[8] ⬢ – SUCACB03,[8] ⬟ – SUCACB05, [9] ▶ – SUCACB06, [10] ◀ – SUCACB08,[23] ○ – SUCACB09,[12] □ – SUCACB10,[11] ◊ – SUCACB11,[12] ● – SUCACB12-17,[13] ♦ – SUCACB18,[24] ■ – SUCACB19, [25] ♦ – SUCACB01,[26] ● – SUCACB04,[9] ■ – SUCACB07[27]; Fumaric acid: ● – FUMAAC,[7] ■ – FUMAAC01[28] ; L-Malic acid: ● – COFRUK10[14]; ■ – COFRUK11 [29]; DL-Malic acid: ♦ – DLMALC11 [30]. Black solid lines correspond to X-ray results obtained in this work. Dashed black lines stand for X-ray results extrapolated using the PBE-D3/PAW thermal expansivities, linearly scaled to reproduce the experimental expansivity at nearly-ambient temperatures. Dashed gray lines stand for X-ray data extrapolated using the extrapolated experimental thermal expansivity, linearly depending on the temperature. Dotted and dash-dotted gray lines stand for X-ray data extrapolated using the PBE-D3/PAW volumes, constantly and linearly scaled to reproduce their experimental counterpart at nearly-ambient temperatures, respectively.

## SI2.4 Calculated quasi-harmonic characteristics

Electron energy – volume curves, discussed in section 4.1, are shown in Figure S5. Magnitude of the vibrational Helmholtz energy clearly depends on the number of the phonon modes per a molecule, being the highest for citric acid and the lowest for pyruvic acid. Shapes of the calculated $A_{vib}(T)$ curves, depicted in Figure S6, exhibiting the steepest descent with temperature for citric acid, confirm this trend.

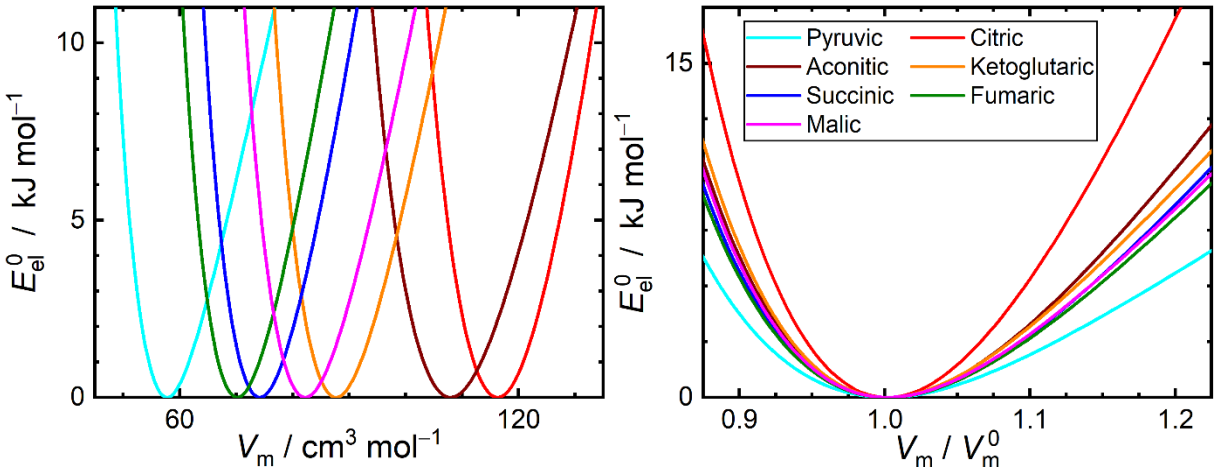


**Figure S5.** Electronic energy – volume curves calculated at the PBE-D3/PAW level of theory. Left – data with respect to the absolute molar volume, emphasizing horizontal shifts of the curves; Right – data with respect to the relative molar volume, emphasizing variation of the slopes of individual curves.

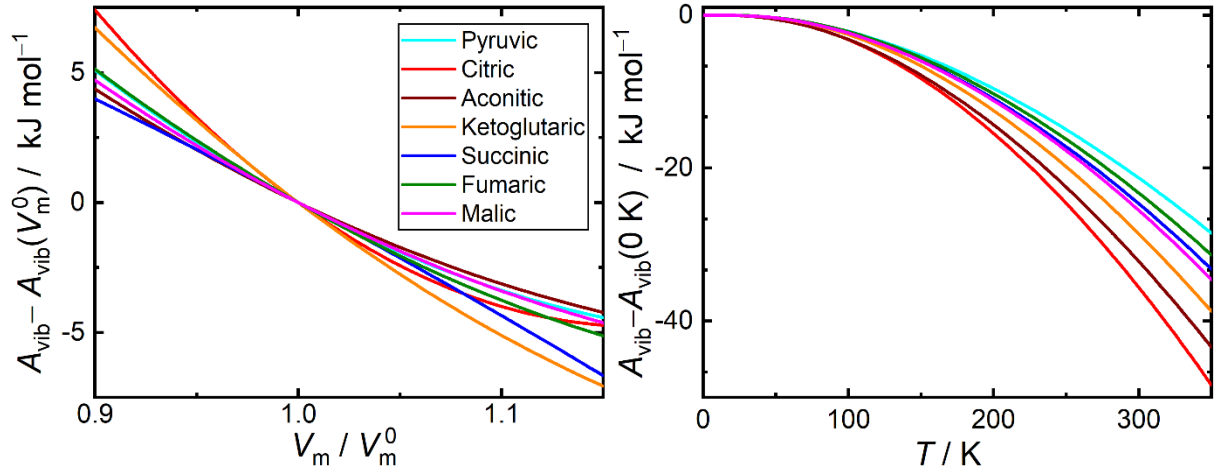


**Figure S6.** Quasi-harmonic vibrational Helmholtz energy calculated at the PBE-D3/PAW level of theory, related to the values obtained for the molar volumes yielding the minimal electronic energy. Left – relative-volume dependent data; Right – temperature dependent data.

## Section SI3 Details on the interpretation of anisotropy of crystals

A correlation between the pair interactions of the closest dimers being oriented in the crystal lattice along the individual crystallographic directions, and the linear thermal expansion coefficients, exhibited by individual crystals in each direction, is depicted in Figure S7. Clearly, there is a significant non-linear correlation between these two descriptors. Materials, for which the three data points lie in proximity in Figure S7, behave rather isotropically, as the hydrogen bonding in those structures occurs diagonally across the unit cells. On the other hand, the four isolated points in the lower left corner in Figure S7 indicate that the hydrogen bonding occurs exclusively along a single crystallographic direction, leading to a considerable material anisotropy. Key components of the pair interaction energies of the closest dimers are listed in Table S3.

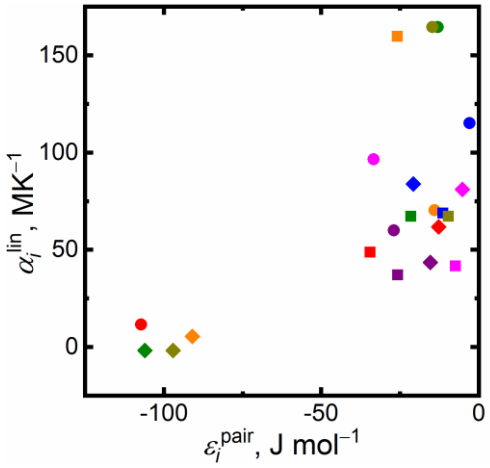


**Figure S7.** Correlation of the linear expansion coefficients $\alpha_i$, valid for the individual crystallographic directions, with the pair interaction energies of the most proximate molecular dimers found in the directions of the individual unit-cell vectors. Color code: red – citric; orange – ketoglutaric; blue – succinic; green – fumaric; magenta – L-malic; purple – DL malic; tan – oxaloacetic. Diamond – direction *a*; square – direction *b*; bullet – direction *c*.

**Table S3.** Calculated sSAPT0/jun-pVDZ interaction energies (kJ mol$^{-1}$) of the closest molecular pairs in the crystals in directions of the crystallographic vectors and their induction and dispersion components.

| Crystal | Direction *a* | | | Direction *b* | | | Direction *c* | | |
|---|---|---|---|---|---|---|---|---|---|
| | $E_{pair}$ | $E_{indu}$ | $E_{disp}$ | $E_{pair}$ | $E_{indu}$ | $E_{disp}$ | $E_{pair}$ | $E_{indu}$ | $E_{disp}$ |
| Citric | -12.7 | -2.0 | -13.8 | -34.4 | -10.0 | -26.4 | -107.2 | -117.6 | -38.2 |
| α-Ketoglutaric | -90.9 | -99.7 | -33.8 | -25.8 | -4.4 | -22.5 | -14.0 | -2.2 | -9.4 |
| Succinic, β | -20.7 | -3.0 | -13.6 | -11.4 | -2.8 | -12.8 | -3.0 | -1.3 | -13.0 |
| Fumaric, α | -105.9 | -102.9 | -33.9 | -21.6 | -6.9 | -13.0 | -13.1 | -2.5 | -18.5 |
| D-Malic, I | -5.2 | -2.8 | -16.9 | -7.4 | -1.5 | -12.8 | -33.4 | -4.5 | -17.9 |
| DL-Malic | -15.4 | -3.1 | -14.9 | -25.7 | -12.2 | -17.7 | -26.9 | -15.7 | -3.1 |
| Oxaloacetic | -97.0 | -102.4 | -35.1 | -9.7 | -1.1 | -10.3 | -14.8 | -2.7 | -12.2 |

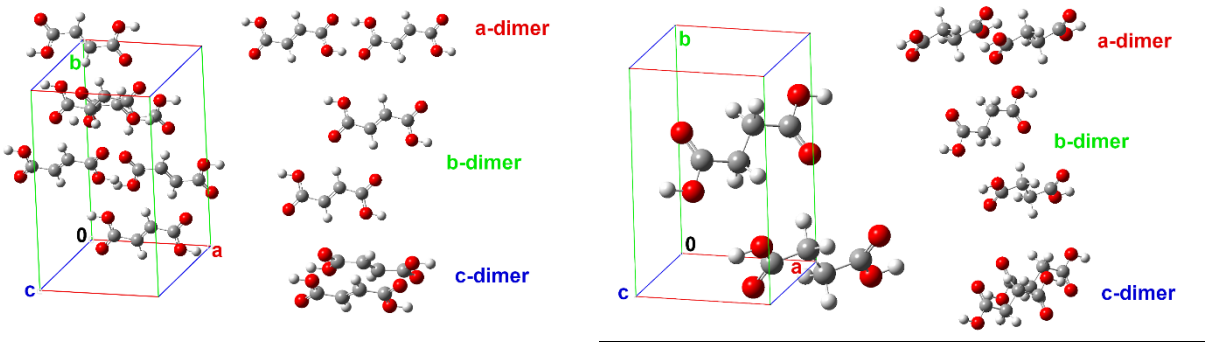


**Figure S8.** Left – crystalline fumaric acid, the different character of its closest dimers along the unit-cell vectors augments the anisotropy of the thermal expansion; Right – crystalline succinic acid, similar character of its closest dimers along the unit-cell vectors attenuates the anisotropy of the thermal expansion.

Extreme cases, exhibiting the strongest and the weakest anisotropy represent crystals of fumaric and succinic acids, respectively. Proximate dimers and their crystallographic orientation are depicted in Figure S8.

For crystalline D,L-malic acid, we suggest that the dominant process is the increase in the inter-layer space allowed by the thermal activation of weaker H-bond interactions involving CH-OH hydroxyl units and COOH groups No. 4 in Figure 4 of the main paper. This process is then accompanied by the increase in intermolecular distances occurring in the perpendicular direction, i.e. within the layers of H-bonded molecules of D,L-malic acid. The observed anisotropy in the thermal expansion of unit cell parameters is further supported by the fact that the hydrogen bonds involving COOH groups at site 1 are thermally inactive keeping thus the intermolecular distance in some directions more or less constant.

## Section SI4 Complete set of $^{1}H$ and $^{13}C$ NMR spectra

Structural anisotropy (section 4.2) was interpreted using the ssNMR spectra, among other. Due to the limited resolution of $^{1}H$ ss-NMR spectra even when measured with $^{1}H$ homodecoupling, we predominantly focused on the analysis of the temperature dependence of $^{13}C$ CP/MAS NMR spectra, which provided significantly better spectral resolution (see Figure S9). Two dimensional $^{1}H$-$^{1}H$ DQ/SQ CRAMPS spectra of the individual acids are presented in Figures S10-S13. Observed $^{1}H$ and $^{13}C$ chemical shifts for crystalline oxaloacetic acid are given in Table S4. Variable-temperature 1H MAS NMR spectra (25 kHz) are presented in Figures S14-S16.

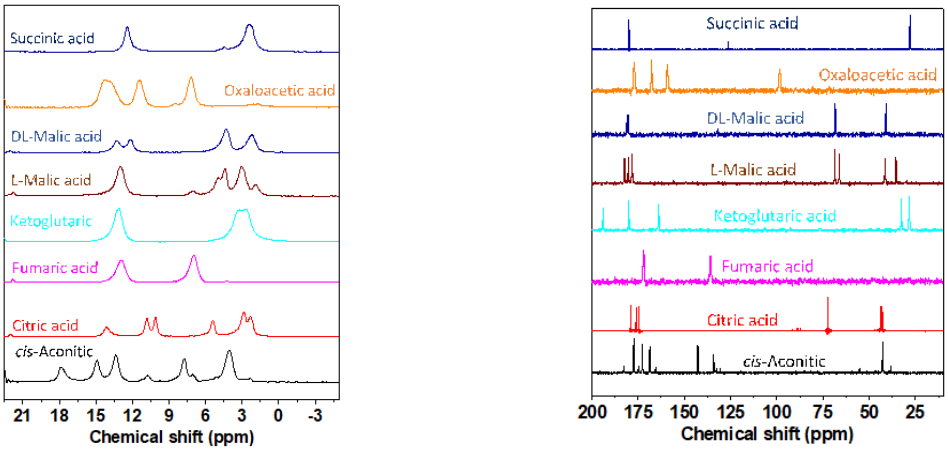


**Figure S9.** $^{1}H$ CRAMPS spectra (left) and $^{13}C$ CP/MAS NMR spectra (right) of carboxylic acids investigated.

### SI4.1 Atomistic interpretation of recorded NMR spectra

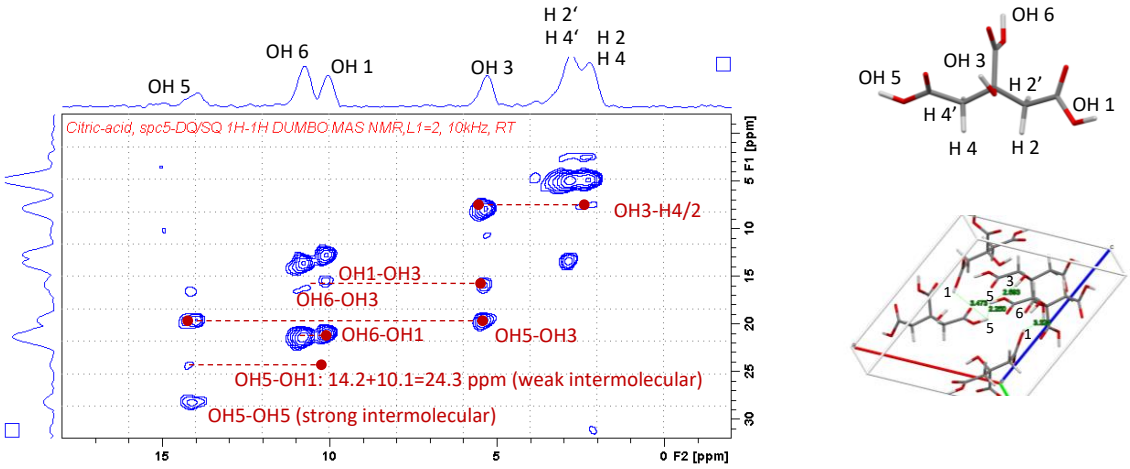


**Figure S10.** $^{1}H$-$^{1}H$ DQ/SQ CRAMPS spectrum and the crystal structure of crystalline citric acid. Specific intermolecular contacts are highlighted both in the spectrum and the crystal structure model.

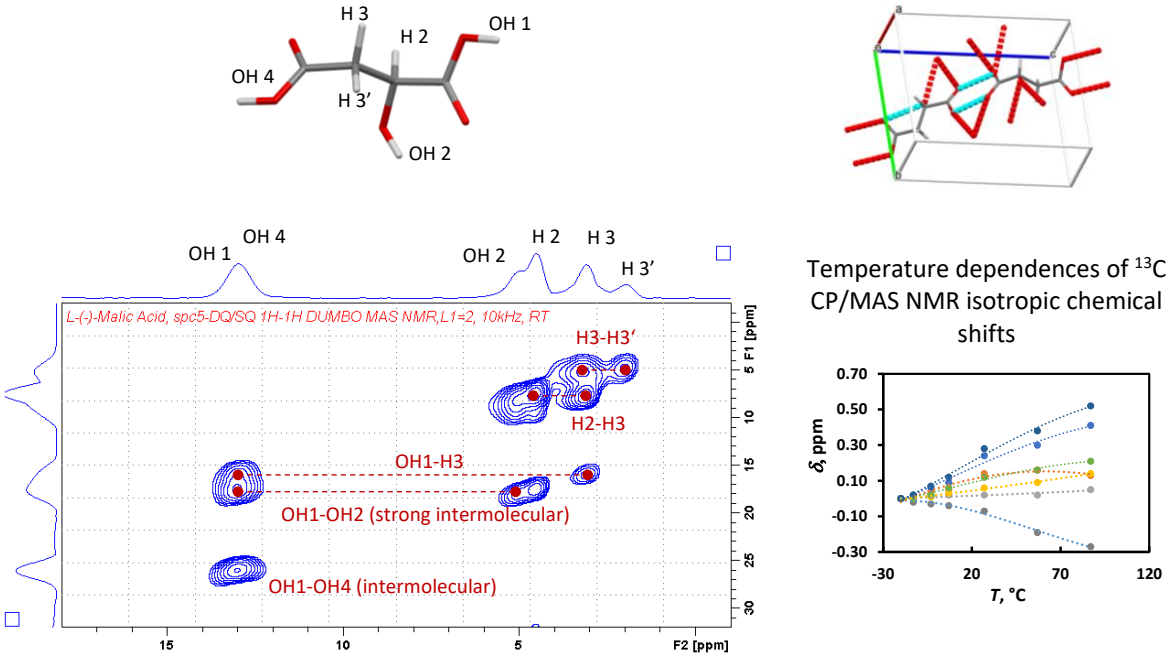


**Figure S11.** $^{1}$H-$^{1}$H DQ/SQ CRAMPS spectrum and the crystal structure of crystalline L-Malic acid. Specific intermolecular contacts are highlighted both in the spectrum and the crystal structure model.

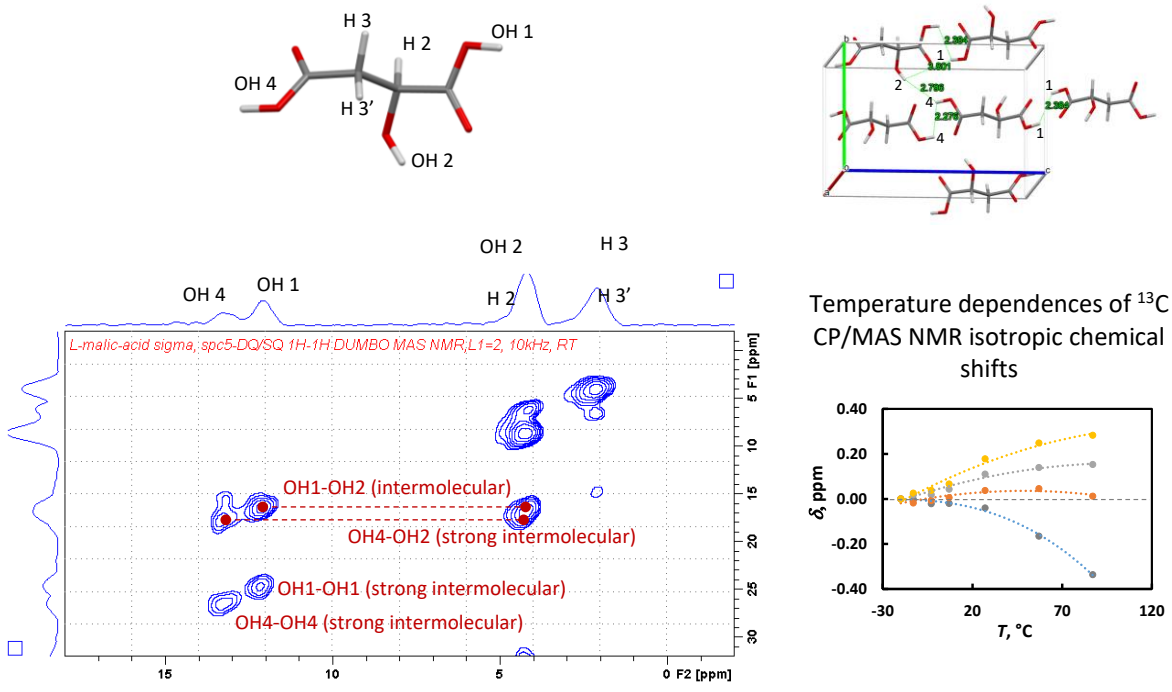


**Figure S12.** $^{1}$H-$^{1}$H DQ/SQ CRAMPS spectrum and the crystal structure of crystalline D,L-malic acid. Specific intermolecular contacts are highlighted both in the spectrum and the crystal structure model.

## SI4.2 Spectral characterization of crystalline oxaloacetic acid

As mentioned above, the analysis of XRPD data recorded for crystalline oxaloacetic acid resulted in the determination of unit cell parameters ($a$=8.69237(14); $b$=6.06857(9); $c$=5.58397(10) Å; $\alpha$=90°; $\beta$=120.8°; $\gamma$=90°, $V$=253 Å$^3$, space group Cm) and four potential crystal structures involving two enol-

and two keto-forms, the *R*-factor of which was nearly identical 2.9-3.2 (Figure S13). Since the positions of the hydrogen atoms could not be directly refined from the recorded XRPD data, we used an NMR crystallography approach based on the comparison of the experimental $^{1}$H and $^{13}$C NMR chemical shifts with the corresponding $^{1}$H and $^{13}$C shielding parameters DFT-calculated for the obtained potential crystal structures. It is now accepted, that correct structure is indicated by the smallest standard deviation (*SD*) values, typically less than 0.5 and 2.5 ppm for the $^{1}$H and $^{13}$C chemical shifts. Such a comparison shown in Figure S13 then clearly identified the most suitable candidate Cm-enol-v2 with *SD*($^{1}$H) = 0.43 ppm and *SD*($^{13}$C) = 1.84 ppm, which is now deposited in the CSD under the Deposition Number 2183126. This enol-form crystal structure is clearly consistent with the recorded relatively high values of NMR chemical shifts (Table S4). In opposite case, e.g. for keto-form the expected NMR chemical shifts of $CH_2$ group should be significantly lower. This structure is also consistent with the expected bond lengths.

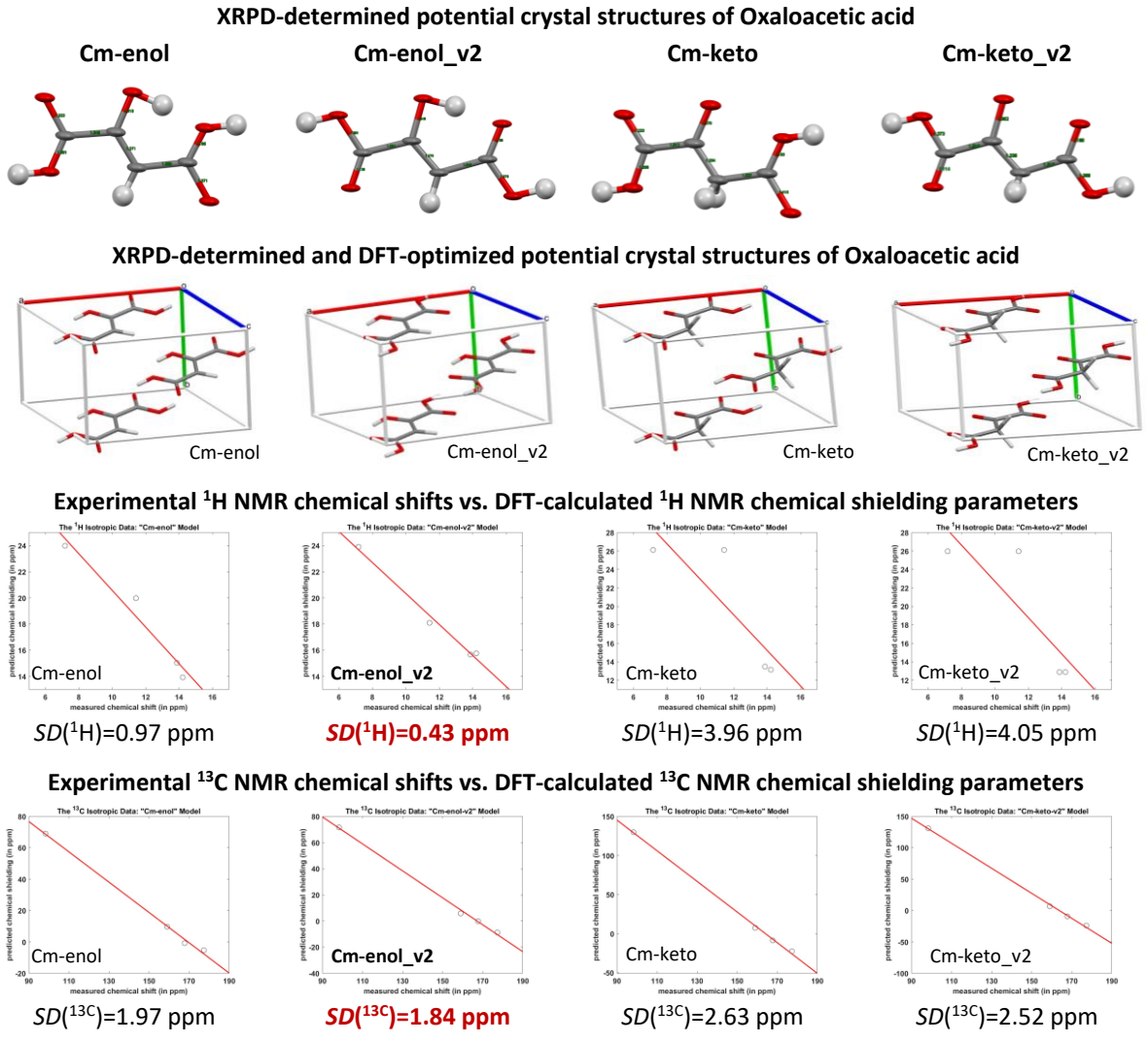


**$^{1}$H-$^{1}$H DQ/SQ CRAMPS spectrum of crystalline oxaloacetic acid in the enol form.**

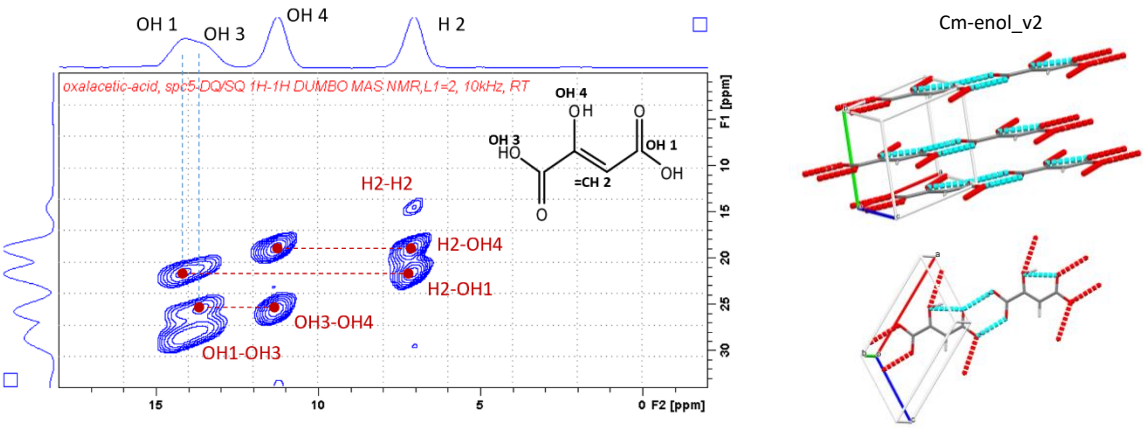


**Figure S13.** $^{1}$H-$^{1}$H DQ/SQ CRAMPS spectrum of crystalline oxaloacetic acid. Specific intermolecular contacts are highlighted in the spectrum.

**Table S4**: Observed $^{1}$H and $^{13}$C chemical shifts for crystalline oxaloacetic acid.

| Atom type | $^{1}$H NMR chemical shifts | Atom type | $^{13}$C NMR chemical shifts |
|---|---|---|---|
| H2 | 7.17 | C2 | 98.35 |
| OH4 | 11.42 | C1 | 177.34 |
| OH3 | 13.87 | C3 | 167.77 |
| OH1 | 14.22 | C4 | 159.04 |

## SI4.3 Variable-temperature 1H MAS NMR spectra (25 kHz)

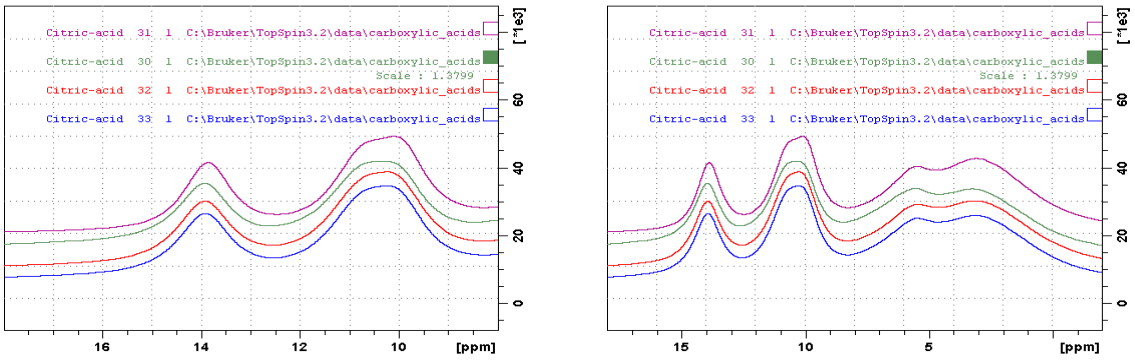


**Figure S14.** Variable temperature $^{1}$H MAS NMR spectra of crystalline citric acid (blue – 270 K; red – 280 K; green – 300 K; purple – 320 K).

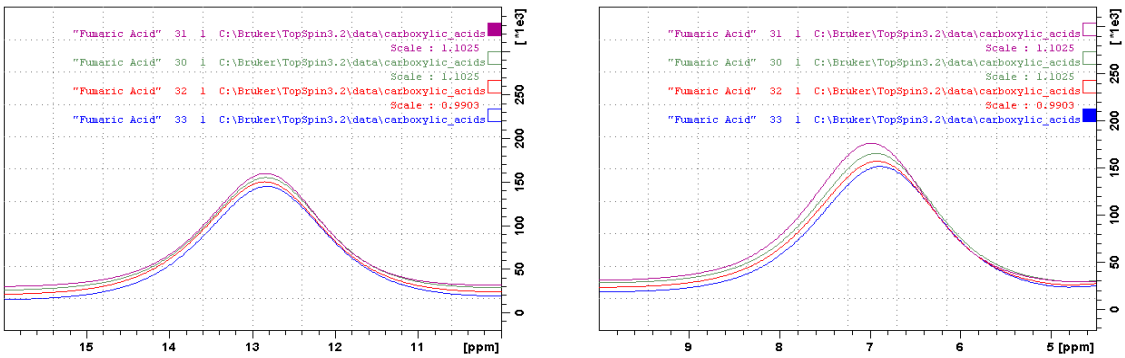


**Figure S15.** Variable temperature $^{1}$H MAS NMR spectra of crystalline fumaric acid (blue – 270 K; red – 280 K; green – 300 K; purple – 320 K).

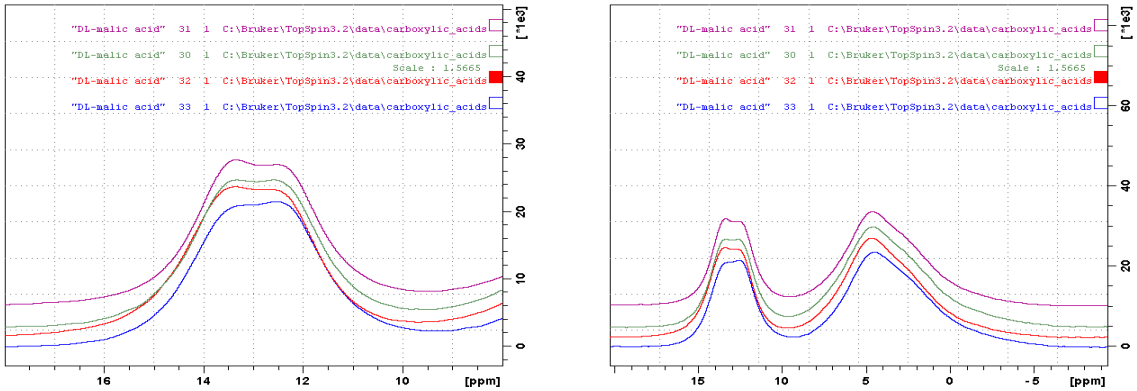


**Figure S16.** Variable temperature $^{1}$H MAS NMR spectra of crystalline D,L-malic acid (blue – 270 K; red – 280 K; green – 300 K; purple – 320 K).

## Section SI5 Analysis of the local segmental dynamics

The observed $^{1}$H spin-lattice relaxation times are summarized in Table S5. The higher the relaxation times are, the more rigid the crystalline structure is, in terms of its local segmental dynamics.

**Table S5**. $^{1}$H spin-lattice relaxation times $T_1(^{1}H)$ and standard deviations (*SD*, in ppm) describing agreement between experimentally determined and DFT calculated isotropic $^{13}$C and $^{1}$H chemical shifts determined for crystalline carboxylic acids.

| | $T_1(^{1}H)$, s | *M*, g/mol | p$K_{a1}$ | *SD* ($^{13}$C)$_{all}$ | *SD* ($^{1}$H)$_{all}$ |
|---|---|---|---|---|---|
| Citric acid | 705 | 192.123 | 3.15 | 1.38 | 0.61 |
| *cis*-Aconitic acid | 34 | 174.108 | 2.8 | 2.63 | 0.67 |
| *α*-Ketoglutaric acid | 483 | 146.11 | NA | 3.24 | 0.51 |
| Succinic acid | 261 | 118.09 | NA | 2.92 | 0.55 |
| Fumaric acid | 206 | 116.07 | 3.03 | 2.11 | 0.11 |
| L-Malic acid | 93 | 134.08 | 3.46 | 5.11 | 0.93 |
| DL-Malic acid | 596 | 134.08 | NA | 2.26 | 0.60 |
| Oxaloacetic acid | 134 | 132.07 | NA | NA | NA |

Comparison of the experimental and DFT calculated isotropic $^{13}$C and $^{1}$H chemical shifts is given in Figures S17 to S19.

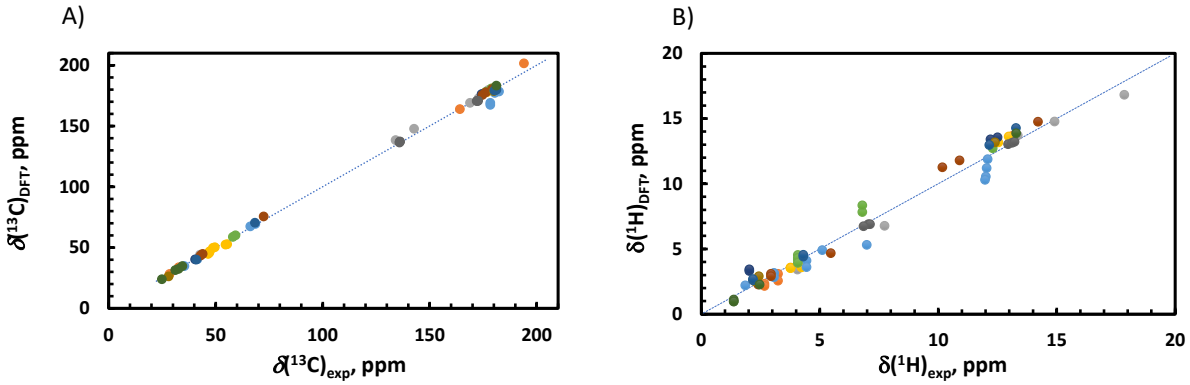


**Figure S17.** Experimentally determined *vs.* DFT-calculated $^{13}$C NMR (A) and $^{1}$H NMR (B) isotropic chemical shifts. Theoretical $^{13}$C and $^{1}$H NMR isotropic chemical shifts $\delta$ were calculated from the isotropic shielding parameter $\sigma$ using the following relations: $\sigma$ ($^{13}$C) = −1.0433·$\delta$($^{13}$C) + 172.82, and $\sigma$ ($^{1}$H) = −1.1677·$\delta$ ($^{1}$H) + 31.095, respectively.

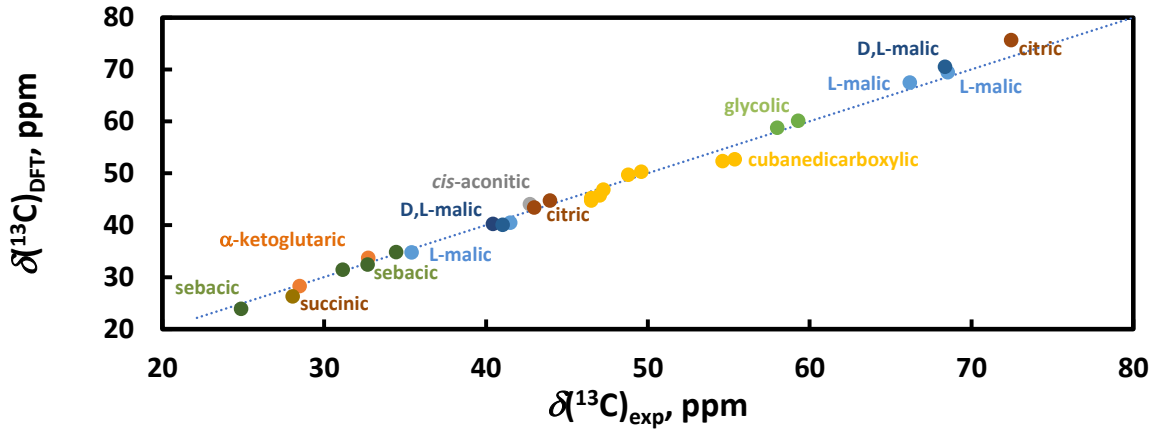

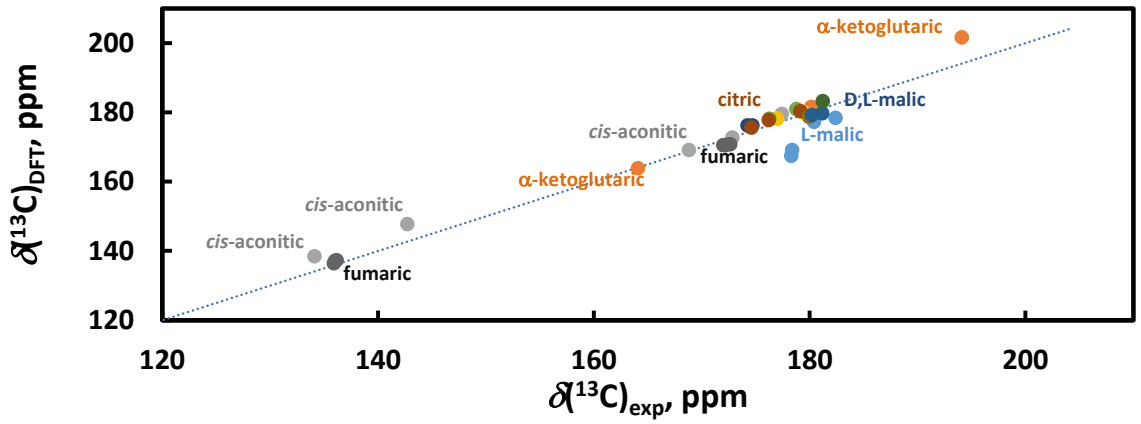


**Figure S18.** Experimentally determined *vs.* DFT-calculated $^{13}$C NMR isotropic chemical shifts – details with assignment of individual dots. Theoretical $^{13}$C isotropic chemical shifts $\delta$ were calculated from the isotropic shielding parameters $\sigma$ using the following relations: $\sigma(^{13}C) = -1.0433 \cdot \delta\,(^{13}C) + 172.82$.

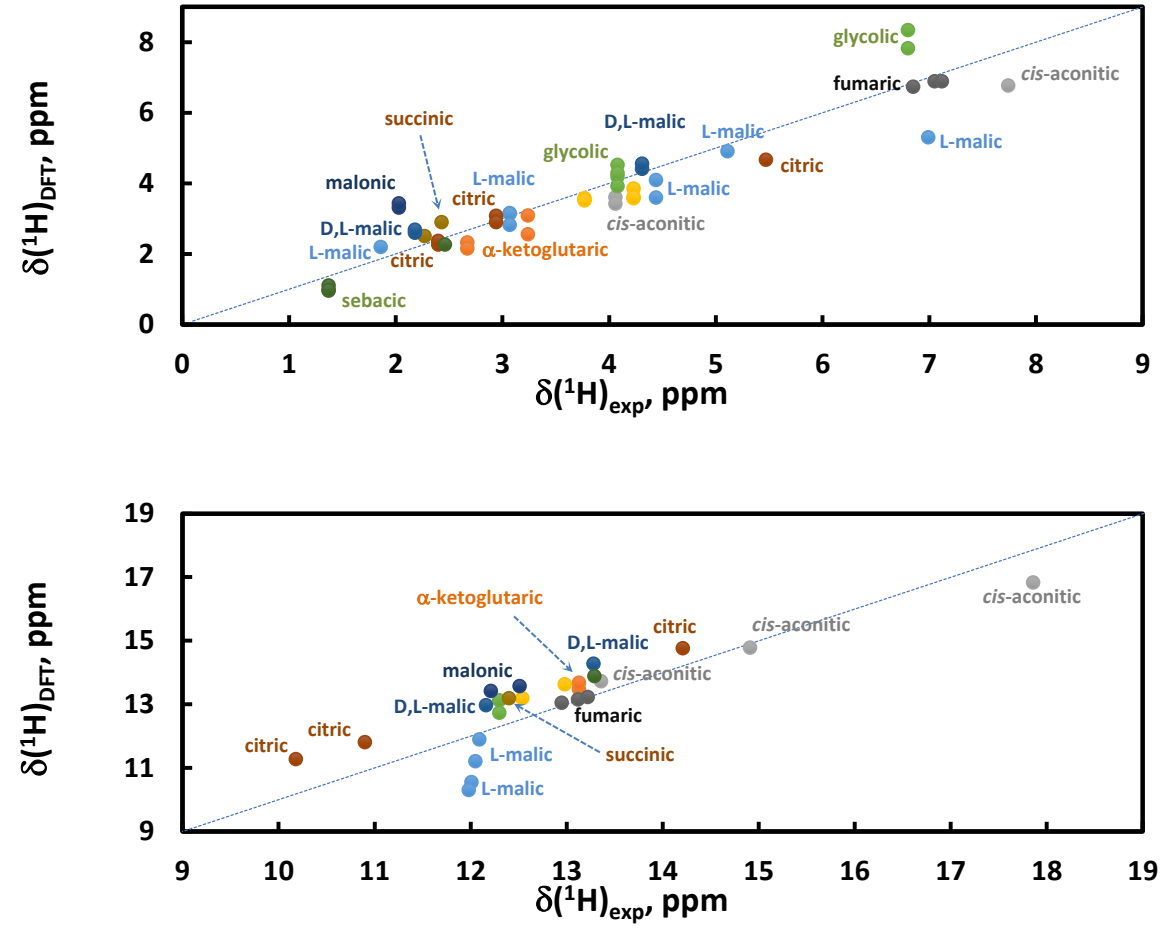


**Figure S19.** Experimentally determined *vs.* DFT-calculated $^{1}$H NMR isotropic chemical shifts – details with assignment of individual dots. Theoretical $^{1}$H NMR isotropic chemical shifts $\delta$ were calculated from the isotropic shielding parameter $\sigma$ using the following relations: $\sigma\,(^{1}H) = -1.1677 \cdot \delta(^{1}H) + 31.095$.

## Section SI6 Discussion of thermodynamic properties of crystalline carboxylic acids

This section discusses phase behavior (SI6.1, as an extension to section 4.4), bulk heat capacities (SI6.2, as an extension to section 4.5) and their computational interpretation (SI6.3) and a protocol for extrapolation of the experimental capacities to sub-ambient temperatures (SI6.4).

### SI6.1 Interlaboratory experimental agreement on phase behavior

Literature values on phase behavior of the studied carboxylic acids are given in Table S6. To our knowledge, no data on isobaric heat capacities and enthalpies of fusion for crystalline cis-aconitic, α-ketoglutaric, L-malic, oxaloacetic, and pyruvic acids exist.

The only paper found in the literature concerning the decomposition of carboxylic acids studied in this work is Wyrzykowski et al.[31] , who studied the decomposition of citric acid and both isomers of aconitic acid. They have performed the measurements at heating rates of 5, 10 and 15 K $min^{-1}$ and an extrapolation of the onset temperatures to the zero heating rate would yield approximately 466 K for citric acid, being in a good agreement with our observation. For cis-aconitic acid, similar extrapolation results in approximately 397 K, 20 K higher than our observations. The reason for this discrepancy is unclear, however the decomposition temperature can be influenced by many factors such as purity of the sample or experimental conditions.

The literature values for $T_{melt}$ of citric acid lie within a somewhat wide range (426 to 434) K. The $T_{melt}$ measured within this work agrees within 1 K with Wilhoit and Shiao[32] and Groen et al.[33]. The literature values for succinic acid lie in a similarly wide range, (455 to 462) K. Our measurements agree within 1 K with Sorum and Durand[34], Lobbia et al.[35] and Roux et al.[36] For fumaric acid, our $T_{melt}$ agrees well with Wilhoit and Shiao,[32] while for enantiopure malic acid, our result is about 4 K higher, in agreement with observation of Leclercq et al.[37] On the other hand, our $T_{melt}$ of α-ketoglutaric acid is about 5 K lower compared to Wilhoit and Lei[38] and Contineanu et al.[39] , which might be due to its fast decomposition at melting. The peak observed on thermograms recorded for oxaloacetic acid was large and irregular and was rather assigned to decomposition, while Fenton and Wilks[40] report melting temperature of *cis*-enol crystal at a similar temperature.

For succinic and *α*-ketoglutaric acid, our $\Delta_{fus}H_m$ values seem to be clearly overstated on the first sight. However, the experiments were replicated and no issues related to calibration were found that could be responsible for so large positive errors. It is also possible that the majority of the available literature values is underestimated, e.g. due to problems related to acquiring pure samples and verifying their purity. Hypothetically, use of the initial mass of a loaded monohydrate sample (from which the water would evaporate during the experiment) in previous works would give errors closely matching the deviation of our $\Delta_{fus}H_m$ values from the literature.

The studied sample of D-malic acid was form I and a transformation to form II [29] or its crystallization was not observed during any of our experiments, as shown in Figure S20. A melted and recrystallized sample exhibited a wide melting peak at an onset temperature with about 10 K lower onset temperature and with about 30 % lower enthalpy. It cannot be definitely decided if the change was solely due to decomposition or if it the phase was melting in the second run was moreover form II.

Controversies about the determination of the α-β-vapor triple point of succinic acid were briefly recalled in some cases,[26, 41] but more often remained unnoticed including several DSC studies, where the transition from the *β* to *α* should be easily detectable (see Figure S21). Another anomaly in the heat capacity of succinic acid that could be assigned to a phase transition was observed by Parks and Huffman[42] around 273 K, but was later assigned to the melting of ice present as an impurity in their sample by Wilhoit et al.[43]

Bruni et al.[44] studied fumaric acid and reported a thermogram with a broad peak with an onset at 494.1 K and a maximum around 530 K interpreted as a sublimation. However, the vapor pressure of fumaric

acid should be only 2 to 12 kPa in this temperature range according to extrapolated measurements by de Kruif et al. [45] and the reported enthalpy 11.8 kJ mol$^{-1}$ is far too small for the sublimation. This ambiguous experiment is later incorrectly interpreted as a melting.[46] In this work, an endothermic but irreversible phase transition from $\alpha$ to $\beta$ form was detected at 477.5 K (Figure S22).

**Table S6.** Temperatures and Enthalpies of Phase transitions and Decomposition

| Reference | $T_g$ / K | $T_{s\rightarrow s}$ / K | $T_{melt}$ / K | $\Delta H_m$ / kJ·mol$^{-1}$ | $T_{decomp}$ / K |
|---|---|---|---|---|---|
| | | | Citric Acid | | |
| Forster et al.[47] | 294.5 | - | 428.8 | 40.3 | - |
| Wilhoit and Shiao[32] | - | - | 426.1 | - | - |
| Tomassetti et al.[48] | - | - | 432.4 | 39.4 | - |
| Klímová and Leitner[49] | - | - | 428.6 | 41.8 | - |
| Wyrzykowski et al.[31] | - | - | 433.9±0.2 | 40.15 | 466[a] |
| Booth et al.[50] | - | - | 427 | 43.46 | - |
| Park et al.[51] | - | - | 430.5 | 45.86 | - |
| Meltzer and Pincu[52] | - | - | 427.80 ± 0.09 | 40.32 ± 0.58 | - |
| Shantikumar et al.[53] | - | - | 428.5 | *83.3* | - |
| Groen et al.[33] | - | - | 426 | - | - |
| **This Work** | **278±3** | - | **426.3±0.3** | **45.3±1.4** | **465** |
| | | | *trans*-Aconitic Acid | | |
| Wilhoit and Lei[38] | - | - | 456.5 | - | 455.8- |
| Wyrzykowski et al.[31] | - | - | - | - | 465[a] |
| **This Work** | - | - | **449.9±2.0** | | **Rapidly at melting** |
| | | | *cis*-Aconitic Acid | | |
| Wyrzykowski et al.[31] | - | - | - | - | 397[a] |
| | | | $\alpha$-Ketoglutraric Acid | | |
| Wilhoit and Lei[38] | - | - | 388.43 | - | - |
| Contineanu et al.[39] | - | - | 388.7 | 28.59 | - |
| **This Work** | - | - | **382.7±1.5** | **33.7±1.0** | **Rapidly in liquid at melting** |
| | | | DL-Malic Acid | | |
| Weiss and Downs[54] | - | - | 401.68 | - | - |
| Wilhoit and Shiao[32] | - | - | 400.4 | - | - |
| Booth et al. [50] | - | - | 403 | 29.03 | - |
| Marques et al.[55] | - | - | 402.9 | - | - |
| Ceolin et al.[56] | - | - | 402 (crI) | 33.5 | - |
| Ceolin et al.[56] | - | - | 396 (crII) | 30.2 | - |
| Leclercq et al.[37] | - | - | 402 | 27.6 | - |
| Zhang et al.[57] | - | - | 403.2 | - | - |
| | | | L-Malic or D-Malic Acid | | |
| Wilhoit and Shiao[32] | - | - | 372.0 | - | - |
| Leclercq et al.[37] | - | - | 376 | 23.0 | - |
| Gao et al.[58] | - | - | 373.87 | 24.795 | - |
| **This Work** | **254±3** | - | **376.1±0.6** | **25.5±0.8** | **455** |
| | | | Oxaloacetic Acid | | |
| Fenton and Wilks[40] | - | - | 425 (*cis*-enol) | - | - |
| Fenton and Wilks[40] | - | - | 457 (*trans*-enol) | - | - |
| Heidelberger[59] | - | - | 424-425 | - | - |
| **This Work** | - | - | - | - | **422** (*trans*-enol) |
| | | | Succinic Acid | | |
| Dupré la Tour[60] | - | 410[b] | - | - | - |
| Rieck[26] | - | - | 460 | - | - |
| Sorum and Durand[34] | - | - | 456 | - | - |
| Wilhoit and Shiao[32] | - | - | 458.9 | - | - |

| Reference | $T_g$ / K | $T_{s\rightarrow s}$ / K | $T_{melt}$ / K | $\Delta H_m$ / kJ·mol$^{-1}$ | $T_{decomp}$ / K |
|---|---|---|---|---|---|
| Morisson and Robertson[61] | - | - | 458 | - | - |
| Wong and Westrum[62] | - | - | 460.9±0.5 | - | - |
| Cingolani and Berchiesi[63] | - | - | 457±0.5 | 32.9±0.3 | - |
| Khetarpal et al.[64] | - | - | 458 | 31.46 | - |
| Ribeiro da Silva et al.[65] | - | - | 457.2 | - | - |
| Roux et al.[36] | - | - | 455.2±1.2 | 34.0±0.3 | - |
| Yu et al.[41] | - | - | 461.8 | 30.04 | - |
| Li et al.[66] | - | - | 458.7 | 32.72 | - |
| Booth et al. [50] | - | - | 458 | 31.26 | - |
| Paluch et al.[67] | - | - | 460.1±0.1 | 27.4±0.4 | - |
| **This Work** | - | **405.2±2.0[b,c]** | **458.3±0.3** | **38.4±1.1** | **Slowly in liquid** |
| | | | Fumaric Acid | | |
| Weiss and Downs[54] | - | - | 557 | - | - |
| Wilhoit and Shiao[32] | - | - | 558.1 | - | - |
| Bruni et al.[44] | - | - | 494.1 | 11.8 | |
| Yang et al.[68] | - | - | 561 | - | - |
| **This Work** | - | **477.3±0.7[d]** | **558.0±2.0** | - | **Rapidly at melting** |
| | | | DL-Malic Acid | | |
| Weiss and Downs[54] | - | - | 401.68 | - | - |
| Wilhoit and Shiao[32] | - | - | 400.4 | - | - |
| Booth et al. [50] | - | - | 403 | 29.03 | - |
| Marques et al.[55] | - | - | 402.9 | - | - |
| Ceolin et al.[56] | - | - | 402 (crI) | 33.5 | - |
| Ceolin et al.[56] | - | - | 396 (crII) | 30.2 | - |
| Leclercq et al.[37] | - | - | 402 | 27.6 | - |
| Zhang et al.[57] | - | - | 403.2 | - | - |
| | | | L-Malic or D-Malic Acid | | |
| Wilhoit and Shiao[32] | - | - | 372.0 | - | - |
| Leclercq et al.[37] | - | - | 376 | 23.0 | - |
| Gao et al.[58] | - | - | 373.87 | 24.795 | - |
| **This Work** | **254±3** | - | **376.1±0.6** | **25.5±0.8** | **455** |
| | | | Oxaloacetic Acid | | |
| Fenton and Wilks[40] | - | - | 425 (*cis*-enol) | - | - |
| Fenton and Wilks[40] | - | - | 457 (*trans*-enol) | - | - |
| Heidelberger[59] | - | - | 424-425 | - | - |
| **This Work** | - | - | - | - | **422** |

[a] Value extrapolated. [b] Transition β→α. [c] Phase transition enthalpy 0.4 ± 0.1 kJ mol$^{-1}$. [d] Phase transition enthalpy α→β 1.7 ± 0.1 kJ mol$^{-1}$.

**SI6.2 Typical thermograms observed in this work**

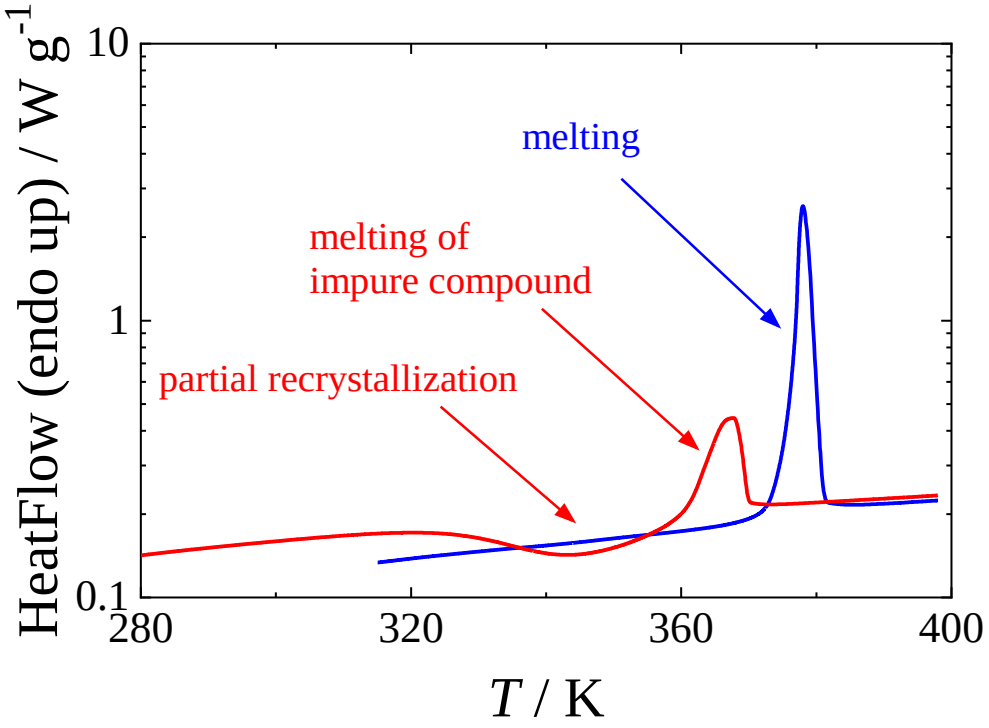


**Figure S20.** Typical thermograms obtained for D-malic acid: —, first run with a dried sample (form I); —, second run (starting with a subcooled liquid sample, probably partially decomposed)

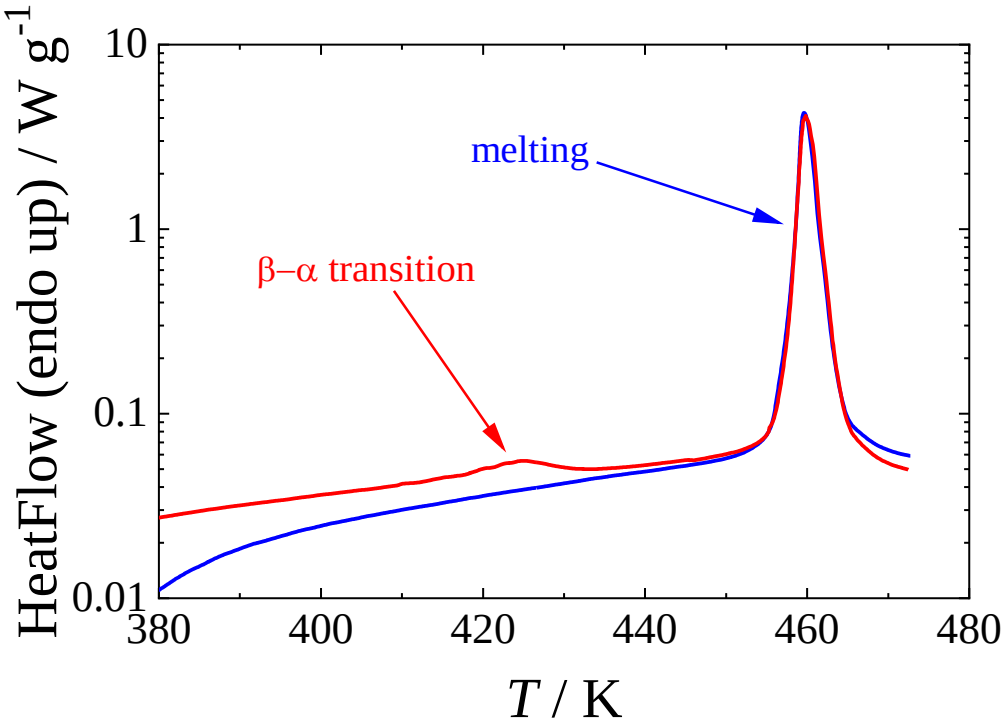


**Figure S21.** Typical thermograms obtained for succinic acid: —, first run with a dried sample ($\beta$ form); —, run with a sample annealed at 423 K ($\alpha$ form).

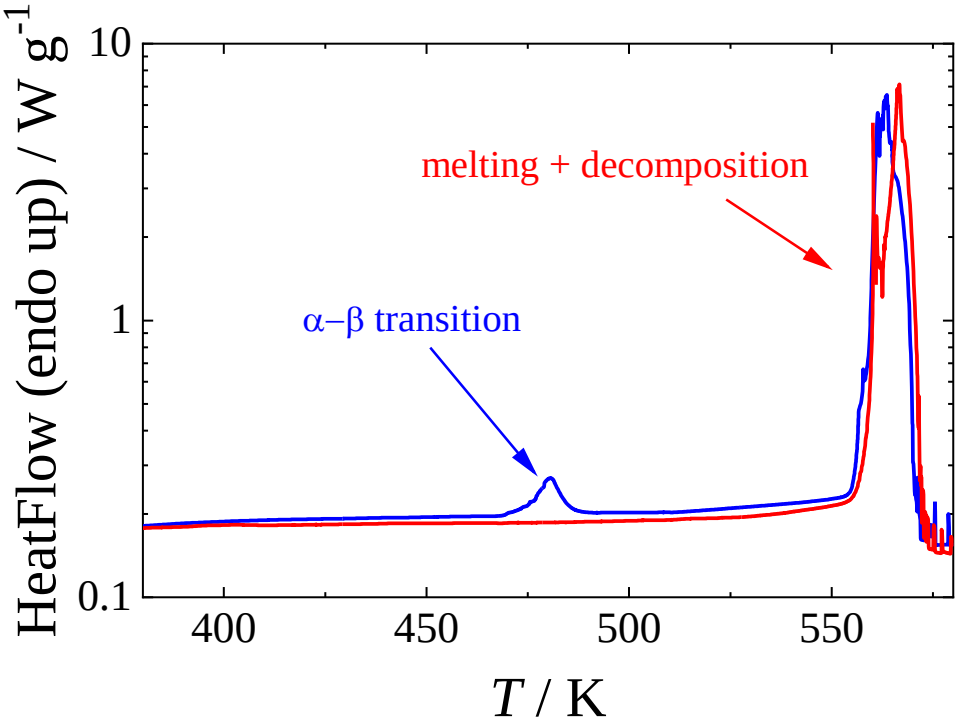


**Figure S22.** Typical thermograms obtained for fumaric acid: —, first run with a dried sample ($\alpha$ form); —, run with a sample annealed at 523 K ($\beta$ form).

## SI6.3 Interlaboratory experimental agreement on heat capacities

Literature studies on heat capacities of the studied acids are summarized in Table S7. Parks and Huffman[42] have measured the heat capacity of succinic and fumaric acid using aneroid calorimetry. For succinic acid, the agreement with our data is within 1% with the exception of a few clear outliers around 273 K (presumably caused by melting of water ice in the sample of Parks and Huffman[42]). For fumaric acid, the agreement is slightly worse (within 2%), but any outlying values due to melting of ice do not occur. De Kruif et al.[45] have measured the heat capacity of citric acid using adiabatic calorimetry and the agreement with our data is excellent (within 0.3%).

**Table S7.** Overview of the literature solid phase heat capacities

| Reference | $N$[a] | ($T_{min}$-$T_{max}$)/K | $u_r(C_{pm})$/%[b] | method |
|---|---|---|---|---|
| Citric Acid | | | | |
| **This work** | **17** | **270-350** | **1.0** | **Tian-Calvet** |
| **This work** | **116** | **1.9-268** | [c] | **Relaxation** |
| de Kruif et al.[45] | 44 | 84-329 | 0.2 | Adiabatic |
| *cis*-Aconitic Acid | | | | |
| **This work** | **14** | **270-335** | **1.0** | **Tian-Calvet** |
| $\alpha$-Ketoglutaric Acid | | | | |
| **This work** | **5** | **270-290** | **1.0** | **Tian-Calvet** |
| D-Malic Acid, form I | | | | |
| **This work** | **16** | **260-335** | **1.0** | **Tian-Calvet** |
| **This work** | **116** | **1.9-268** | [c] | **Relaxation** |
| Oxaloacetic Acid | | | | |
| **This work** | **17** | **270-350** | **1.0** | **Tian-Calvet** |
| **This work** | **116** | **1.9-268** | [c] | **Relaxation** |
| Succinic Acid, $\beta$-phase | | | | |
| **This work** | **17** | **270-350** | **1.0** | **Tian-Calvet** |
| Parks and Huffman[42] | 16 | 93-290 | 1.0 | Aneroid |
| Vanderzee and Westrum[69] | 88 | 5.2-323 | 0.1 | Adiabatic |
| Succinic Acid, $\alpha$-phase | | | | |
| **This work** | **20** | **260-355** | **1.0** | **Tian-Calvet** |
| **This work** | **128** | **2.0-268** | [c] | **Relaxation** |
| Fumaric Acid, $\alpha$-phase | | | | |
| **This work** | **17** | **270-350** | **1.0** | **Tian-Calvet** |
| **This work** | **116** | **1.9-268** | [c] | **Relaxation** |
| Parks and Huffman[42] | 16 | 91-297 | 1.0 | Aneroid |
| Fumaric Acid, $\beta$–phase | | | | |
| **This work** | **20** | **260-355** | **1.0** | **Tian-Calvet** |
| **This work** | **126** | **2.0-260** | [c] | **Relaxation** |
| D-Malic Acid, form I | | | | |
| **This work** | **16** | **260-335** | **1.0** | **Tian-Calvet** |
| **This work** | **116** | **1.9-268** | [c] | **Relaxation** |
| Oxaloacetic Acid | | | | |
| **This work** | **17** | **270-350** | **1.0** | **Tian-Calvet** |
| **This work** | **116** | **1.9-268** | [c] | **Relaxation** |

[a] $N$ = number of data points. References in bold were included in the correlation.
[b] $u_r(C_{pm})$ stands for relative uncertainty in heat capacity as stated by the authors.
[c] For specification of $u_r(C_{pm})$ of PPMS using thermal relaxation measurement technique, see Tables S9 to S14.

The succinic acid sample of Vanderzee and Westrum[69] was purified by sublimation, which gives $\alpha$-phase according to Yu et al.[41] However, we received a mixture of the polymorphs by the same process,

which slowly turned to practically pure $\beta$-phase. To resolve the ambiguity, we measured heat capacities of both phases with SETARAM μDSC IIIa and find out that they differ noticeably in their trend. Heat capacity of $\beta$-phase is higher and steeper at ambient temperatures. Based on the comparison, we suggest that Vanderzee and Westrum[69] studied $\beta$-phase most probably (or a mixture with a dominant share of this polymorph) and therefore Quantum Design PPMS was only used to determine heat capacities of $\alpha$-phase.

Experimental heat capacities obtained in this work with SETARAM μDSC IIIa and Quantum Design PPMS are listed in Tables S8 to S14. The selected experimental and literature data given in bold in Table S7 were fitted with eqs. SI1 and SI2 whose parameters are given in Table S15. For $\alpha$-ketoglutaric and cis-aconitic acid, some of the parameters were fixed as zero to avoid overfitting of the data. Deviation plots for the respective experimental heat capacity data are shown in Figure S23.

**Table S8**: Experimental isobaric heat capacities of crystalline (if not specified otherwise) carboxylic acids $C_{p,\mathrm{m}}$ obtained using SETARAM μDSC IIIa.

| $T$ / K | $C_{p,\mathrm{m}}^{\mathrm{exp}}$ [a] / J K$^{-1}$ mol$^{-1}$ at $p$ = (100 ± 5) kPa | | | | | | | | | |
|---|---|---|---|---|---|---|---|---|---|---|
| | Citric | cis-Aconitic | $\alpha$-Keto-glutaric | Succinic, $\beta$ | Succinic, $\alpha$ | Fumaric, $\alpha$ | Fumaric, $\beta$ | D-Malic | Oxalo-acetic | Pyruvic, liquid |
| 260 | | | | | 134.96 | | 129.26 | 147.49 | | |
| 265 | | | | | 137.03 | | 131.12 | 149.81 | | 189.42 |
| 270 | 209.24 | 186.21 | 171.00 | 141.25 | 139.14 | 132.59 | 133.00 | 152.22 | 141.41 | 188.66 |
| 275 | 212.11 | 188.92 | 173.21 | 143.52 | 141.21 | 134.45 | 134.82 | 154.72 | 143.49 | 187.90 |
| 280 | 214.94 | 191.65 | 175.31 | 145.68 | 143.27 | 136.19 | 136.62 | 157.43 | 145.61 | 187.14 |
| 285 | 217.81 | 194.38 | 177.60 | 147.83 | 145.34 | 137.94 | 138.41 | 160.12 | 147.70 | 186.38 |
| 290 | 220.72 | 196.92 | 180.16 | 150.03 | 147.38 | 139.69 | 140.17 | 162.58 | 149.69 | |
| 295 | 223.76 | 199.42 | | 152.21 | 149.40 | 141.45 | 141.89 | 164.97 | 151.68 | |
| 300 | 226.80 | 201.90 | | 154.48 | 151.41 | 143.22 | 143.59 | 167.41 | 153.76 | |
| 305 | 229.67 | 204.53 | | 157.13 | 153.42 | 145.34 | 145.31 | 169.70 | 155.94 | |
| 310 | 232.30 | 207.05 | | 159.33 | 155.58 | 147.04 | 147.11 | 172.02 | 157.82 | |
| 315 | 235.07 | 209.81 | | 161.56 | 157.77 | 148.97 | 148.96 | 174.38 | 159.85 | |
| 320 | 238.03 | 212.76 | | 164.15 | 159.97 | 150.36 | 150.80 | 176.79 | 162.13 | |
| 325 | 240.94 | 216.61 | | 166.34 | 162.22 | 151.93 | 152.63 | 179.32 | 164.35 | |
| 330 | 243.96 | 220.78 | | 168.61 | 164.49 | 153.60 | 154.49 | 182.04 | 166.58 | |
| 335 | 246.98 | 225.31 | | 171.09 | 166.77 | 155.37 | 156.36 | 185.16 | 168.74 | |
| 340 | 249.85 | | | 173.57 | 169.02 | 157.03 | 158.17 | | 170.73 | |
| 345 | 252.72 | | | 176.09 | 171.22 | 158.71 | 159.94 | | 172.45 | |
| 350 | 255.51 | | | 178.88 | 173.47 | 160.65 | 161.72 | | 174.18 | |
| 355 | | | | | 175.80 | | 163.50 | | | |

[a] Standard uncertainty of temperature is $u(T)$ = 0.05 K, and the combined expanded uncertainty of the heat capacity is $U_{\mathrm{c}}\left(C_{p,\mathrm{m}}\right) = 0.01 C_{p,\mathrm{m}}$ (0.95 level of confidence).

**Table S9**: Experimental heat capacity of Citric acid (in J $K^{-1}$ $mol^{-1}$) obtained using QuantumDesign PPMS.[a]

| $T$ / K | $C_{pm}^{o}$ [c] | $\delta_{rel}$ [b]/ % | $T$ / K | $C_{pm}^{o}$ [c] | $\delta_{rel}$ [b]/ % | $T$ / K | $C_{pm}^{o}$ [c] | $\delta_{rel}$ [b]/ % |
|---|---|---|---|---|---|---|---|---|
| 1.91 | 0.0062288 | −2.33% | 30.11 | 21.832 | 0.01% | 141.81 | 128.45 | 0.04% |
| 1.91 | 0.0062298 | −2.31% | 35.15 | 28.788 | −0.24% | 141.88 | 128.16 | −0.23% |
| 2.19 | 0.0097600 | 0.91% | 35.15 | 28.805 | −0.19% | 148.78 | 133.37 | 0.16% |
| 2.19 | 0.0097703 | 1.02% | 40.22 | 35.791 | −0.10% | 148.85 | 132.99 | −0.17% |
| 2.55 | 0.015760 | 2.16% | 40.23 | 35.785 | −0.16% | 155.77 | 138.25 | 0.28% |
| 2.55 | 0.015776 | 2.26% | 45.26 | 42.562 | 0.23% | 155.87 | 137.69 | −0.17% |
| 3.01 | 0.025813 | 0.55% | 45.28 | 42.522 | 0.08% | 162.80 | 142.84 | 0.23% |
| 3.01 | 0.025812 | 0.54% | 50.32 | 48.841 | 0.18% | 162.87 | 142.57 | 0.00% |
| 3.60 | 0.044467 | −0.42% | 50.32 | 48.843 | 0.18% | 169.82 | 147.50 | 0.26% |
| 3.60 | 0.044457 | −0.44% | 55.37 | 54.811 | 0.20% | 169.88 | 147.38 | 0.15% |
| 4.27 | 0.076550 | −0.72% | 55.37 | 54.818 | 0.21% | 176.82 | 152.03 | 0.25% |
| 4.27 | 0.076835 | −0.58% | 60.43 | 60.392 | −0.02% | 176.87 | 151.83 | 0.10% |
| 5.16 | 0.14180 | −1.33% | 60.43 | 60.408 | 0.00% | 183.82 | 156.29 | 0.11% |
| 5.16 | 0.14221 | −1.17% | 65.46 | 65.840 | 0.01% | 183.86 | 156.08 | −0.05% |
| 6.24 | 0.27062 | 0.21% | 65.46 | 65.769 | −0.10% | 190.82 | 160.57 | 0.01% |
| 6.29 | 0.27611 | −0.71% | 70.53 | 71.093 | 0.04% | 190.85 | 160.40 | −0.11% |
| 7.69 | 0.54851 | 1.38% | 70.57 | 71.015 | −0.14% | 197.82 | 164.83 | −0.08% |
| 7.73 | 0.55768 | 1.19% | 75.57 | 76.162 | 0.15% | 197.84 | 164.70 | −0.17% |
| 9.89 | 1.2322 | 0.17% | 75.62 | 76.080 | −0.02% | 204.81 | 169.25 | −0.05% |
| 9.89 | 1.2315 | 0.04% | 80.60 | 81.238 | 0.54% | 204.83 | 169.11 | −0.14% |
| 11.91 | 2.2122 | 0.46% | 80.65 | 81.135 | 0.35% | 211.81 | 173.67 | 0.00% |
| 11.93 | 2.2108 | 0.01% | 85.65 | 86.049 | 0.77% | 211.81 | 173.58 | −0.05% |
| 13.95 | 3.5058 | −0.39% | 85.70 | 85.917 | 0.56% | 218.80 | 178.25 | 0.15% |
| 13.95 | 3.5065 | −0.37% | 90.71 | 90.453 | 0.72% | 218.81 | 178.36 | 0.21% |
| 15.95 | 5.0813 | −0.47% | 90.75 | 90.371 | 0.58% | 225.79 | 182.60 | 0.18% |
| 15.95 | 5.0847 | −0.44% | 95.75 | 94.506 | 0.48% | 225.80 | 182.40 | 0.07% |
| 18.01 | 6.9881 | −0.13% | 95.81 | 94.327 | 0.24% | 232.78 | 186.62 | 0.05% |
| 18.01 | 6.9862 | −0.16% | 100.78 | 98.340 | 0.18% | 232.79 | 186.75 | 0.12% |
| 20.02 | 9.1040 | 0.43% | 100.79 | 98.403 | 0.24% | 239.77 | 190.75 | −0.01% |
| 20.04 | 9.1280 | 0.47% | 106.82 | 102.94 | 0.01% | 239.79 | 190.81 | 0.01% |
| 22.05 | 11.384 | 0.32% | 106.88 | 102.82 | −0.15% | 246.76 | 194.71 | −0.15% |
| 22.06 | 11.382 | 0.22% | 113.82 | 108.27 | −0.02% | 246.79 | 194.84 | −0.09% |
| 24.06 | 13.803 | 0.08% | 113.86 | 108.20 | −0.11% | 253.75 | 198.78 | −0.22% |
| 24.09 | 13.730 | −0.65% | 120.81 | 113.63 | 0.12% | 253.78 | 198.90 | −0.16% |
| 26.09 | 16.410 | 0.11% | 120.87 | 113.38 | −0.13% | 260.74 | 202.94 | −0.23% |
| 26.09 | 16.427 | 0.22% | 127.82 | 118.66 | 0.07% | 260.77 | 203.12 | −0.15% |
| 28.09 | 19.095 | 0.16% | 127.89 | 118.47 | −0.13% | 267.72 | 207.38 | −0.09% |
| 28.12 | 19.071 | −0.16% | 134.80 | 123.65 | 0.10% | 267.76 | 207.50 | −0.05% |
| 30.11 | 21.833 | 0.02% | 134.86 | 123.36 | −0.17% | | | |

[a] Standard uncertainty of temperature is $u(T)$=0.004 K, and the combined expanded uncertainty of heat capacity $U_c(C_{pm})$ with 0.95 level of confidence ($k$=2) is: $U_c(C_{pm})$=0.1 $C_{pm}$ below 10 K; $U_c(C_{pm})$=0.03 $C_{pm}$ in temperature range (10 to 40) K; $U_c(C_{pm})$=0.02 $C_{pm}$ in temperature range (40 to 300) K. Values are reported with more digits than is justified by the experimental uncertainty to avoid round-off errors in calculations based on these results. Measurements are performed in vacuum (residual pressure $p<10^{-4}$ Pa).

[b] $\delta_{rel}$ is the percentage deviation of experimental heat capacity data from the smoothed values from equations SI1 and SI2 with parameters from Table S15.

**Table S10**: Experimental heat capacity of Succinic acid ($\alpha$–phase, in J $K^{-1}$ $mol^{-1}$) obtained using QuantumDesign PPMS.[a]

| $T$ / K | $C_{pm}^{o}$ [c] | $\delta_{rel}$ [b]/ % | $T$ / K | $C_{pm}^{o}$ [c] | $\delta_{rel}$ [b]/ % | $T$ / K | $C_{pm}^{o}$ [c] | $\delta_{rel}$ [b]/ % |
|---|---|---|---|---|---|---|---|---|
| 1.98 | 0.0059308 | -1.36% | 21.90 | 7.5550 | -1.23% | 127.64 | 82.386 | -0.01% |
| 1.98 | 0.0059535 | -0.98% | 23.77 | 9.3160 | -0.46% | 127.86 | 82.255 | -0.29% |
| 1.99 | 0.0059594 | -1.17% | 23.81 | 9.3321 | -0.65% | 134.67 | 85.494 | 0.15% |
| 2.25 | 0.0086736 | 0.22% | 25.74 | 11.211 | -0.50% | 134.88 | 85.378 | -0.09% |
| 2.25 | 0.0086600 | 0.07% | 25.78 | 11.228 | -0.71% | 141.66 | 88.334 | 0.07% |
| 2.25 | 0.0086993 | 0.13% | 27.81 | 13.259 | -0.82% | 141.89 | 88.204 | -0.18% |
| 2.58 | 0.012938 | 0.00% | 27.86 | 13.306 | -0.83% | 148.68 | 91.110 | -0.03% |
| 2.58 | 0.012925 | -0.11% | 29.75 | 15.269 | -0.73% | 148.92 | 90.965 | -0.29% |
| 2.58 | 0.013040 | 0.44% | 29.85 | 15.341 | -0.93% | 155.66 | 93.929 | -0.02% |
| 2.99 | 0.019994 | 0.13% | 34.80 | 20.741 | 0.25% | 155.91 | 93.761 | -0.31% |
| 2.99 | 0.020051 | 0.42% | 34.91 | 20.815 | 0.03% | 162.69 | 96.846 | 0.09% |
| 3.00 | 0.020134 | 0.44% | 39.91 | 26.211 | 0.91% | 162.94 | 96.681 | -0.18% |
| 3.45 | 0.030484 | 0.72% | 40.02 | 26.272 | 0.71% | 169.74 | 99.800 | 0.25% |
| 3.45 | 0.030528 | 0.52% | 44.97 | 31.309 | 0.70% | 170.00 | 99.620 | -0.03% |
| 3.45 | 0.030490 | 0.31% | 45.09 | 31.349 | 0.45% | 176.70 | 102.50 | 0.21% |
| 4.07 | 0.050725 | 2.20% | 50.02 | 36.212 | 0.60% | 176.96 | 102.27 | -0.12% |
| 4.07 | 0.050220 | 1.18% | 50.14 | 36.239 | 0.35% | 183.91 | 105.11 | 0.00% |
| 4.07 | 0.050347 | 1.21% | 55.09 | 40.872 | 0.53% | 184.19 | 105.14 | -0.07% |
| 4.82 | 0.082622 | -0.03% | 55.22 | 40.880 | 0.27% | 190.89 | 107.90 | 0.06% |
| 4.82 | 0.082643 | -0.01% | 60.13 | 44.920 | -0.15% | 191.16 | 107.73 | -0.19% |
| 4.83 | 0.082715 | -0.05% | 60.27 | 44.879 | -0.49% | 197.95 | 110.72 | 0.12% |
| 5.72 | 0.13767 | -1.05% | 65.14 | 48.881 | -0.21% | 198.23 | 110.52 | -0.16% |
| 5.72 | 0.13773 | -1.06% | 65.27 | 48.700 | -0.78% | 204.91 | 113.57 | 0.24% |
| 5.72 | 0.13728 | -1.39% | 70.29 | 52.477 | -0.58% | 205.18 | 113.44 | 0.03% |
| 7.27 | 0.28582 | -2.28% | 70.43 | 52.416 | -0.88% | 211.90 | 116.48 | 0.39% |
| 7.27 | 0.28598 | -2.48% | 75.35 | 56.002 | -0.41% | 212.18 | 116.23 | 0.08% |
| 7.28 | 0.28722 | -2.26% | 75.49 | 55.952 | -0.66% | 218.91 | 119.46 | 0.58% |
| 8.46 | 0.47319 | 0.25% | 80.37 | 59.427 | 0.06% | 219.20 | 119.22 | 0.28% |
| 8.52 | 0.48565 | 0.67% | 80.52 | 59.359 | -0.21% | 225.91 | 121.91 | 0.33% |
| 8.57 | 0.49270 | 0.28% | 85.43 | 62.689 | 0.52% | 226.21 | 121.66 | 0.02% |
| 9.74 | 0.72177 | -1.19% | 85.57 | 62.610 | 0.27% | 232.90 | 124.56 | 0.24% |
| 9.74 | 0.72118 | -1.27% | 90.53 | 65.535 | 0.58% | 233.18 | 124.35 | -0.02% |
| 11.72 | 1.2933 | -0.06% | 90.69 | 65.472 | 0.35% | 239.90 | 127.21 | 0.14% |
| 11.72 | 1.2914 | -0.23% | 95.54 | 68.019 | 0.41% | 240.20 | 126.96 | -0.15% |
| 13.77 | 2.1300 | 1.13% | 95.70 | 67.925 | 0.14% | 246.92 | 129.90 | 0.06% |
| 13.77 | 2.1347 | 1.34% | 100.59 | 70.374 | 0.20% | 247.21 | 129.63 | -0.24% |
| 15.71 | 3.1239 | 0.86% | 100.77 | 70.189 | -0.18% | 253.92 | 132.68 | 0.04% |
| 15.71 | 3.1590 | 1.96% | 106.66 | 73.211 | 0.16% | 254.23 | 132.39 | -0.27% |
| 17.72 | 4.4798 | 2.83% | 106.86 | 73.094 | -0.13% | 260.91 | 135.62 | 0.14% |
| 17.77 | 4.4592 | 1.52% | 113.68 | 76.389 | 0.12% | 261.22 | 135.30 | -0.19% |
| 19.80 | 5.8922 | 0.00% | 113.88 | 76.295 | -0.12% | 267.92 | 138.80 | 0.38% |
| 19.83 | 5.9669 | 0.88% | 120.63 | 79.367 | 0.00% | 268.23 | 138.33 | -0.05% |
| 21.83 | 7.5513 | -0.42% | 120.84 | 79.238 | -0.28% | | | |

[a] Standard uncertainty of temperature is $u(T)$=0.004 K, and the combined expanded uncertainty of heat capacity $U_c(C_{pm})$ with 0.95 level of confidence ($k$=2) is: $U_c(C_{pm})$=0.1 $C_{pm}$ below 10 K; $U_c(C_{pm})$=0.03 $C_{pm}$ in temperature range (10 to 40) K; $U_c(C_{pm})$=0.02 $C_{pm}$ in temperature range (40 to 300) K. Values are reported with more digits than is justified by the experimental uncertainty to avoid round-off errors in calculations based on these results. Measurements are performed in vacuum (residual pressure $p<10^{-4}$ Pa).

[b] $\delta_{rel}$ is the percentage deviation of experimental heat capacity data from the smoothed values from equations SI1 and SI2 with parameters from Table S15.

**Table S11**: Experimental heat capacity of Fumaric acid ($\alpha$–phase, in J $K^{-1}$ $mol^{-1}$) obtained using QuantumDesign PPMS.[a]

| $T$ / K | $C_{pm}^{o}$ [c] | $\delta_{rel}$ [b]/ % | $T$ / K | $C_{pm}^{o}$ [c] | $\delta_{rel}$ [b]/ % | $T$ / K | $C_{pm}^{o}$ [c] | $\delta_{rel}$ [b]/ % |
|---|---|---|---|---|---|---|---|---|
| 1.91 | 0.0084250 | -1.74% | 30.11 | 15.227 | -0.11% | 141.86 | 84.956 | -0.01% |
| 1.91 | 0.0084310 | -1.67% | 35.17 | 20.211 | -0.16% | 141.91 | 84.806 | -0.21% |
| 2.19 | 0.012955 | 0.64% | 35.17 | 20.208 | -0.17% | 148.84 | 87.759 | 0.05% |
| 2.19 | 0.012972 | 0.78% | 40.24 | 25.187 | 0.03% | 148.90 | 87.565 | -0.20% |
| 2.56 | 0.020509 | 1.78% | 40.24 | 25.182 | -0.02% | 155.84 | 90.560 | 0.13% |
| 2.56 | 0.020501 | 1.62% | 45.28 | 29.934 | 0.15% | 155.91 | 90.380 | -0.10% |
| 3.02 | 0.032891 | 0.69% | 45.29 | 30.001 | 0.32% | 162.85 | 93.349 | 0.22% |
| 3.02 | 0.032934 | 0.82% | 50.34 | 34.479 | 0.29% | 162.91 | 93.202 | 0.04% |
| 3.60 | 0.054429 | 0.03% | 50.34 | 34.454 | 0.21% | 169.84 | 96.107 | 0.31% |
| 3.60 | 0.054402 | -0.10% | 55.39 | 38.682 | 0.10% | 169.91 | 95.964 | 0.13% |
| 4.28 | 0.088919 | -0.38% | 55.39 | 38.677 | 0.08% | 176.86 | 98.775 | 0.31% |
| 4.28 | 0.088874 | -0.43% | 60.45 | 42.593 | -0.23% | 176.92 | 98.634 | 0.14% |
| 5.17 | 0.15059 | -1.34% | 60.45 | 42.594 | -0.23% | 183.86 | 101.26 | 0.15% |
| 5.17 | 0.15037 | -1.48% | 65.48 | 46.363 | -0.25% | 183.92 | 101.07 | -0.06% |
| 6.26 | 0.26028 | -0.67% | 65.48 | 46.370 | -0.23% | 190.87 | 103.88 | 0.15% |
| 6.26 | 0.25999 | -0.87% | 70.54 | 49.934 | -0.25% | 190.91 | 103.73 | -0.02% |
| 7.71 | 0.47629 | 0.58% | 70.58 | 49.883 | -0.41% | 197.86 | 106.33 | 0.00% |
| 7.75 | 0.48492 | 0.69% | 75.60 | 53.394 | -0.04% | 197.90 | 106.19 | -0.14% |
| 9.90 | 0.96210 | 0.14% | 75.63 | 53.264 | -0.32% | 204.86 | 108.94 | 0.01% |
| 9.91 | 0.96447 | 0.02% | 80.62 | 56.698 | 0.27% | 204.89 | 108.80 | -0.13% |
| 11.95 | 1.6257 | 0.13% | 80.65 | 56.642 | 0.13% | 211.86 | 111.56 | 0.05% |
| 11.95 | 1.6218 | -0.14% | 85.68 | 59.762 | 0.42% | 211.88 | 111.44 | -0.07% |
| 13.95 | 2.4816 | 0.10% | 85.72 | 59.693 | 0.26% | 218.85 | 114.33 | 0.22% |
| 13.96 | 2.4813 | 0.07% | 90.74 | 62.627 | 0.52% | 218.86 | 114.27 | 0.16% |
| 15.97 | 3.5427 | 0.07% | 90.77 | 62.552 | 0.37% | 225.84 | 116.78 | 0.12% |
| 15.97 | 3.5394 | -0.09% | 95.79 | 65.110 | 0.26% | 225.85 | 116.82 | 0.15% |
| 17.97 | 4.8173 | 0.57% | 95.82 | 65.020 | 0.09% | 232.84 | 119.32 | 0.10% |
| 17.99 | 4.8047 | 0.10% | 100.81 | 67.400 | -0.05% | 232.84 | 119.24 | 0.03% |
| 20.03 | 6.2766 | 0.36% | 100.81 | 67.447 | 0.02% | 239.84 | 121.78 | 0.03% |
| 20.03 | 6.2739 | 0.32% | 106.86 | 70.225 | -0.08% | 239.84 | 121.67 | -0.07% |
| 22.06 | 7.8577 | 0.01% | 106.89 | 70.068 | -0.33% | 246.83 | 124.08 | -0.17% |
| 22.08 | 7.8660 | -0.04% | 113.84 | 73.343 | -0.09% | 246.84 | 124.20 | -0.07% |
| 24.08 | 9.5489 | -0.33% | 113.88 | 73.176 | -0.34% | 253.82 | 126.50 | -0.25% |
| 24.10 | 9.5745 | -0.25% | 120.83 | 76.389 | -0.02% | 253.84 | 126.61 | -0.17% |
| 26.11 | 11.3810 | -0.30% | 120.89 | 76.197 | -0.30% | 260.81 | 129.05 | -0.23% |
| 26.11 | 11.4120 | -0.10% | 127.83 | 79.316 | 0.01% | 260.83 | 129.10 | -0.19% |
| 28.13 | 13.3320 | 0.07% | 127.89 | 79.151 | -0.23% | 267.79 | 131.72 | -0.10% |
| 28.13 | 13.3320 | 0.07% | 134.85 | 82.122 | -0.05% | 267.82 | 131.80 | -0.05% |
| 30.11 | 15.2400 | -0.02% | 134.90 | 81.978 | -0.25% | | | |

[a] Standard uncertainty of temperature is $u(T)$=0.004 K, and the combined expanded uncertainty of heat capacity $U_c(C_{pm})$ with 0.95 level of confidence ($k$=2) is: $U_c(C_{pm})$=0.1 $C_{pm}$ below 10 K; $U_c(C_{pm})$=0.03 $C_{pm}$ in temperature range (10 to 40) K; $U_c(C_{pm})$=0.02 $C_{pm}$ in temperature range (40 to 300) K. Values are reported with more digits than is justified by the experimental uncertainty to avoid round-off errors in calculations based on these results. Measurements are performed in vacuum (residual pressure $p<10^{-4}$ Pa).

[b] $\delta_{rel}$ is the percentage deviation of experimental heat capacity data from the smoothed values from equations SI1 and SI2 with parameters from Table S15.

**Table S12**: Experimental heat capacity of Fumaric acid ($\beta$–phase, in J $K^{-1}$ $mol^{-1}$) obtained using QuantumDesign PPMS.[a]

| $T$ / K | $C_{pm}^{o}$ [c] | $\delta_{rel}$ [b]/ % | $T$ / K | $C_{pm}^{o}$ [c] | $\delta_{rel}$ [b]/ % | $T$ / K | $C_{pm}^{o}$ [c] | $\delta_{rel}$ [b]/ % |
|---|---|---|---|---|---|---|---|---|
| 1.98 | 0.011322 | -0.83% | 21.95 | 8.1423 | 0.06% | 120.52 | 76.848 | -0.04% |
| 1.98 | 0.011321 | -0.84% | 21.98 | 8.1266 | -0.43% | 120.64 | 76.637 | -0.37% |
| 1.99 | 0.011366 | -0.87% | 23.97 | 9.8701 | -0.13% | 127.50 | 79.773 | -0.08% |
| 2.26 | 0.016486 | -0.20% | 23.99 | 9.8562 | -0.50% | 127.61 | 79.546 | -0.42% |
| 2.26 | 0.016494 | -0.16% | 25.96 | 11.704 | -0.01% | 134.48 | 82.635 | -0.11% |
| 2.27 | 0.016596 | 0.09% | 26.02 | 11.721 | -0.27% | 134.60 | 82.365 | -0.49% |
| 2.61 | 0.024664 | -0.02% | 27.97 | 13.633 | 0.14% | 141.47 | 85.444 | -0.12% |
| 2.61 | 0.024697 | 0.12% | 27.98 | 13.673 | 0.37% | 141.57 | 85.237 | -0.41% |
| 2.62 | 0.024796 | 0.09% | 29.97 | 15.555 | -0.01% | 148.45 | 88.383 | 0.07% |
| 3.05 | 0.038135 | 0.19% | 30.00 | 15.661 | 0.46% | 148.53 | 88.026 | -0.37% |
| 3.05 | 0.038128 | 0.17% | 34.98 | 20.537 | -0.01% | 155.50 | 91.207 | 0.14% |
| 3.05 | 0.038357 | 0.31% | 35.05 | 20.544 | -0.29% | 155.57 | 90.944 | -0.17% |
| 3.54 | 0.058382 | 0.85% | 40.05 | 25.545 | 0.11% | 162.48 | 94.024 | 0.28% |
| 3.54 | 0.058615 | 1.01% | 40.10 | 25.613 | 0.19% | 162.57 | 93.745 | -0.06% |
| 3.54 | 0.058662 | 1.01% | 45.11 | 30.246 | -0.07% | 169.44 | 96.849 | 0.45% |
| 4.19 | 0.094735 | 1.39% | 45.18 | 30.224 | -0.35% | 169.54 | 96.316 | -0.14% |
| 4.20 | 0.094742 | 1.26% | 50.14 | 34.836 | 0.33% | 176.47 | 99.301 | 0.24% |
| 4.20 | 0.094979 | 1.51% | 50.21 | 34.798 | 0.04% | 176.54 | 99.271 | 0.19% |
| 4.99 | 0.15361 | 0.61% | 55.19 | 39.067 | 0.36% | 183.49 | 101.93 | 0.25% |
| 4.99 | 0.15339 | 0.41% | 55.27 | 39.011 | 0.05% | 183.51 | 101.89 | 0.20% |
| 4.99 | 0.15348 | 0.47% | 60.24 | 42.860 | -0.12% | 190.46 | 104.49 | 0.22% |
| 5.94 | 0.25022 | -0.42% | 60.32 | 42.789 | -0.41% | 190.48 | 104.38 | 0.11% |
| 5.94 | 0.25043 | -0.48% | 65.25 | 46.604 | -0.09% | 197.44 | 106.83 | 0.01% |
| 5.94 | 0.25044 | -0.48% | 65.33 | 46.504 | -0.42% | 197.45 | 106.72 | -0.10% |
| 7.38 | 0.46218 | -1.26% | 70.29 | 50.115 | -0.14% | 204.42 | 109.32 | -0.05% |
| 7.38 | 0.46170 | -1.59% | 70.37 | 50.020 | -0.44% | 204.42 | 109.37 | 0.00% |
| 7.39 | 0.46335 | -1.39% | 75.33 | 53.513 | -0.02% | 211.40 | 112.02 | 0.09% |
| 8.67 | 0.73803 | 0.00% | 75.41 | 53.321 | -0.48% | 211.43 | 111.88 | -0.04% |
| 8.71 | 0.74891 | -0.03% | 80.37 | 56.889 | 0.38% | 218.38 | 114.95 | 0.44% |
| 8.75 | 0.75516 | -0.25% | 80.46 | 56.750 | 0.03% | 218.39 | 114.77 | 0.28% |
| 9.83 | 1.0503 | 0.30% | 85.41 | 60.140 | 0.82% | 225.36 | 117.23 | 0.22% |
| 9.83 | 1.0445 | -0.40% | 85.51 | 59.956 | 0.42% | 225.36 | 117.22 | 0.21% |
| 11.86 | 1.7423 | -0.46% | 90.48 | 63.026 | 0.87% | 232.34 | 119.88 | 0.33% |
| 11.87 | 1.7556 | 0.08% | 90.56 | 62.854 | 0.51% | 232.34 | 119.75 | 0.22% |
| 13.85 | 2.6493 | 0.47% | 95.50 | 65.476 | 0.50% | 239.32 | 122.10 | 0.09% |
| 13.85 | 2.6365 | -0.13% | 95.59 | 65.272 | 0.11% | 239.32 | 122.24 | 0.20% |
| 15.86 | 3.7436 | 0.16% | 100.51 | 67.688 | 0.00% | 246.31 | 124.48 | -0.02% |
| 15.87 | 3.7464 | 0.16% | 100.63 | 67.508 | -0.36% | 246.32 | 124.30 | -0.17% |
| 17.92 | 5.0449 | -0.20% | 106.56 | 70.525 | -0.11% | 253.28 | 126.90 | -0.08% |
| 17.93 | 5.0514 | -0.29% | 106.68 | 70.299 | -0.51% | 253.30 | 126.75 | -0.20% |
| 19.94 | 6.5594 | 0.49% | 113.53 | 73.723 | -0.11% | 260.25 | 129.46 | -0.03% |
| 19.95 | 6.5770 | 0.66% | 113.64 | 73.493 | -0.49% | 260.26 | 129.24 | -0.20% |

[a] Standard uncertainty of temperature is $u(T)$=0.004 K, and the combined expanded uncertainty of heat capacity $U_c(C_{pm})$ with 0.95 level of confidence ($k$=2) is: $U_c(C_{pm})$=0.1 $C_{pm}$ below 10 K; $U_c(C_{pm})$=0.03 $C_{pm}$ in temperature range (10 to 40) K; $U_c(C_{pm})$=0.02 $C_{pm}$ in temperature range (40 to 300) K. Values are reported with more digits than is justified by the experimental uncertainty to avoid round-off errors in calculations based on these results. Measurements are performed in vacuum (residual pressure $p<10^{-4}$ Pa).

[b] $\delta_{rel}$ is the percentage deviation of experimental heat capacity data from the smoothed values from equations SI1 and SI2 with parameters from Table S15.

**Table S13**: Experimental heat capacity of D-Malic acid, form I (in J $K^{-1}$ $mol^{-1}$) obtained using QuantumDesign PPMS.[a]

| $T$ / K | $C_{pm}^{o}$ [c] | $\delta_{rel}$ [b]/ % | $T$ / K | $C_{pm}^{o}$ [c] | $\delta_{rel}$ [b]/ % | $T$ / K | $C_{pm}^{o}$ [c] | $\delta_{rel}$ [b]/ % |
|---|---|---|---|---|---|---|---|---|
| 1.91 | 0.0093406 | -0.82% | 30.04 | 16.881 | -0.26% | 141.80 | 94.758 | 0.09% |
| 1.91 | 0.0093483 | -0.74% | 35.09 | 22.301 | 0.05% | 141.86 | 94.532 | -0.18% |
| 2.19 | 0.013579 | 0.55% | 35.09 | 22.300 | 0.04% | 148.80 | 97.899 | 0.08% |
| 2.19 | 0.013582 | 0.45% | 40.17 | 27.771 | 0.56% | 148.88 | 97.678 | -0.18% |
| 2.54 | 0.020484 | 0.92% | 40.17 | 27.770 | 0.55% | 155.84 | 101.08 | 0.13% |
| 2.54 | 0.020470 | 0.85% | 45.22 | 33.017 | 0.67% | 155.91 | 100.87 | -0.11% |
| 2.99 | 0.031782 | 0.05% | 45.22 | 33.040 | 0.74% | 162.80 | 104.31 | 0.26% |
| 2.99 | 0.031793 | 0.08% | 50.29 | 38.003 | 0.49% | 162.89 | 103.89 | -0.18% |
| 3.56 | 0.051679 | -0.72% | 50.29 | 38.013 | 0.51% | 169.83 | 107.39 | 0.23% |
| 3.57 | 0.051704 | -0.75% | 55.33 | 42.674 | 0.17% | 169.91 | 107.15 | -0.02% |
| 4.22 | 0.084732 | -0.67% | 55.33 | 42.654 | 0.12% | 176.85 | 110.50 | 0.24% |
| 4.22 | 0.084665 | -0.82% | 60.41 | 47.037 | -0.27% | 176.92 | 110.35 | 0.08% |
| 5.09 | 0.14609 | -2.03% | 60.41 | 47.006 | -0.34% | 183.87 | 113.59 | 0.23% |
| 5.09 | 0.14636 | -2.03% | 65.44 | 51.230 | -0.38% | 183.93 | 113.39 | 0.03% |
| 6.16 | 0.26078 | -1.08% | 65.44 | 51.199 | -0.45% | 190.87 | 116.60 | 0.16% |
| 6.16 | 0.26114 | -0.99% | 70.50 | 55.201 | -0.45% | 190.92 | 116.42 | -0.02% |
| 7.68 | 0.51611 | 1.62% | 70.56 | 55.065 | -0.79% | 197.87 | 119.68 | 0.14% |
| 7.72 | 0.52289 | 1.12% | 75.54 | 59.041 | -0.29% | 197.91 | 119.43 | -0.09% |
| 9.86 | 1.0585 | 0.39% | 75.61 | 58.914 | -0.59% | 204.86 | 122.74 | 0.10% |
| 9.87 | 1.0567 | 0.01% | 80.56 | 62.831 | 0.16% | 204.92 | 122.48 | -0.14% |
| 11.89 | 1.8036 | 0.51% | 80.63 | 62.637 | -0.23% | 211.86 | 125.95 | 0.17% |
| 11.89 | 1.8038 | 0.50% | 85.63 | 66.350 | 0.43% | 211.90 | 125.79 | 0.02% |
| 13.88 | 2.7754 | 0.69% | 85.69 | 66.169 | 0.09% | 218.86 | 129.18 | 0.23% |
| 13.88 | 2.7748 | 0.67% | 90.70 | 69.562 | 0.51% | 218.89 | 129.10 | 0.16% |
| 15.90 | 3.9992 | 1.00% | 90.76 | 69.446 | 0.30% | 225.85 | 132.24 | 0.16% |
| 15.92 | 4.0248 | 1.38% | 95.74 | 72.452 | 0.41% | 225.89 | 132.15 | 0.08% |
| 17.96 | 5.4186 | 0.03% | 95.82 | 72.191 | -0.01% | 232.85 | 135.36 | 0.11% |
| 17.96 | 5.4360 | 0.34% | 100.79 | 75.021 | 0.08% | 232.88 | 135.19 | -0.02% |
| 19.97 | 7.0338 | 0.11% | 100.79 | 75.054 | 0.12% | 239.86 | 138.42 | 0.01% |
| 19.99 | 7.0645 | 0.27% | 106.82 | 78.125 | -0.03% | 239.88 | 138.28 | -0.10% |
| 22.01 | 8.7691 | -0.69% | 106.89 | 77.953 | -0.29% | 246.86 | 141.51 | -0.09% |
| 22.01 | 8.8009 | -0.37% | 113.80 | 81.646 | -0.01% | 246.87 | 141.31 | -0.24% |
| 24.02 | 10.676 | -0.60% | 113.87 | 81.425 | -0.32% | 253.86 | 144.43 | -0.32% |
| 24.03 | 10.664 | -0.79% | 120.83 | 85.118 | 0.10% | 253.87 | 144.57 | -0.22% |
| 26.04 | 12.693 | -0.53% | 120.89 | 84.957 | -0.12% | 260.86 | 147.71 | -0.31% |
| 26.04 | 12.703 | -0.45% | 127.80 | 88.414 | 0.14% | 260.86 | 147.88 | -0.19% |
| 28.04 | 14.774 | -0.34% | 127.88 | 88.255 | -0.08% | 267.84 | 151.18 | -0.19% |
| 28.05 | 14.762 | -0.49% | 134.80 | 91.550 | 0.05% | 267.85 | 151.22 | -0.16% |
| 30.04 | 16.878 | -0.28% | 134.88 | 91.281 | -0.28% | | | |

[a] Standard uncertainty of temperature is $u(T)$=0.004 K, and the combined expanded uncertainty of heat capacity $U_c(C_{pm})$ with 0.95 level of confidence ($k$=2) is: $U_c(C_{pm})$=0.1 $C_{pm}$ below 10 K; $U_c(C_{pm})$=0.03 $C_{pm}$ in temperature range (10 to 40) K; $U_c(C_{pm})$=0.02 $C_{pm}$ in temperature range (40 to 300) K. Values are reported with more digits than is justified by the experimental uncertainty to avoid round-off errors in calculations based on these results. Measurements are performed in vacuum (residual pressure $p<10^{-4}$ Pa).

[b] $\delta_{rel}$ is the percentage deviation of experimental heat capacity data from the smoothed values from equations SI1 and SI2 with parameters from Table S15.

**Table S14**: Experimental heat capacity of Oxaloacetic acid (in J $K^{-1}$ $mol^{-1}$) obtained using QuantumDesign PPMS.[a]

| $T$ / K | $C_{pm}^{o}$ [c] | $\delta_{rel}$ [b]/ % | $T$ / K | $C_{pm}^{o}$ [c] | $\delta_{rel}$ [b]/ % | $T$ / K | $C_{pm}^{o}$ [c] | $\delta_{rel}$ [b]/ % |
|---|---|---|---|---|---|---|---|---|
| 1.91 | 0.017638 | 0.65% | 30.08 | 16.519 | 0.08% | 141.80 | 87.869 | -0.15% |
| 1.91 | 0.017619 | 0.54% | 35.12 | 21.760 | 0.51% | 141.89 | 87.442 | -0.68% |
| 2.19 | 0.024273 | 0.36% | 35.14 | 21.713 | 0.21% | 148.81 | 90.979 | -0.04% |
| 2.19 | 0.024274 | 0.36% | 40.20 | 26.845 | 0.31% | 148.92 | 90.480 | -0.64% |
| 2.55 | 0.034601 | -0.12% | 40.20 | 26.844 | 0.29% | 155.83 | 94.193 | 0.20% |
| 2.55 | 0.034639 | -0.01% | 45.25 | 31.753 | 0.38% | 155.92 | 93.733 | -0.33% |
| 3.00 | 0.050662 | -1.21% | 45.26 | 31.775 | 0.45% | 162.84 | 97.335 | 0.37% |
| 3.00 | 0.050685 | -1.16% | 50.30 | 36.293 | 0.28% | 162.92 | 96.956 | -0.05% |
| 3.58 | 0.077708 | -1.18% | 50.30 | 36.257 | 0.17% | 169.84 | 100.46 | 0.54% |
| 3.58 | 0.077812 | -1.05% | 55.36 | 40.471 | 0.02% | 169.90 | 100.11 | 0.17% |
| 4.28 | 0.12503 | 1.00% | 55.36 | 40.430 | -0.09% | 176.84 | 103.35 | 0.49% |
| 4.29 | 0.12496 | 0.52% | 60.41 | 44.300 | -0.34% | 176.92 | 102.91 | 0.03% |
| 5.11 | 0.19702 | 0.11% | 60.42 | 44.241 | -0.48% | 183.84 | 106.22 | 0.42% |
| 5.11 | 0.19734 | 0.22% | 65.45 | 48.065 | -0.25% | 183.89 | 105.87 | 0.07% |
| 6.19 | 0.33619 | 1.14% | 65.45 | 47.992 | -0.41% | 190.85 | 109.00 | 0.28% |
| 6.26 | 0.34178 | -0.44% | 70.52 | 51.590 | -0.27% | 190.91 | 108.63 | -0.08% |
| 7.59 | 0.59453 | 1.00% | 70.57 | 51.395 | -0.72% | 197.84 | 111.83 | 0.21% |
| 7.62 | 0.60263 | 1.34% | 75.56 | 54.999 | -0.09% | 197.88 | 111.55 | -0.05% |
| 9.88 | 1.2058 | -0.25% | 75.62 | 54.723 | -0.67% | 204.84 | 114.66 | 0.14% |
| 9.88 | 1.2070 | -0.20% | 80.58 | 58.502 | 0.56% | 204.87 | 114.38 | -0.11% |
| 11.91 | 2.0020 | 0.73% | 80.65 | 58.187 | -0.06% | 211.83 | 117.69 | 0.25% |
| 11.92 | 1.9980 | 0.27% | 85.64 | 61.695 | 0.88% | 211.88 | 117.40 | -0.01% |
| 13.93 | 2.9771 | 0.09% | 85.71 | 61.445 | 0.41% | 218.83 | 120.91 | 0.51% |
| 13.93 | 2.9785 | 0.14% | 90.69 | 64.659 | 1.06% | 218.86 | 120.64 | 0.28% |
| 15.93 | 4.1459 | -0.05% | 90.77 | 64.178 | 0.24% | 225.82 | 123.74 | 0.45% |
| 15.93 | 4.1458 | -0.09% | 95.74 | 67.107 | 0.64% | 225.84 | 123.45 | 0.21% |
| 17.99 | 5.5530 | -0.09% | 95.81 | 66.745 | 0.05% | 232.82 | 126.66 | 0.45% |
| 17.99 | 5.5573 | -0.03% | 100.78 | 69.417 | 0.23% | 232.83 | 126.36 | 0.21% |
| 20.02 | 7.1290 | 0.19% | 100.78 | 69.456 | 0.28% | 239.82 | 129.07 | 0.06% |
| 20.02 | 7.1333 | 0.24% | 106.81 | 72.133 | -0.12% | 239.82 | 129.30 | 0.24% |
| 22.04 | 8.7767 | -0.34% | 106.89 | 71.709 | -0.76% | 246.82 | 131.97 | 0.06% |
| 22.05 | 8.7553 | -0.72% | 113.81 | 75.500 | -0.04% | 246.84 | 131.63 | -0.21% |
| 24.07 | 10.551 | -0.75% | 113.88 | 75.128 | -0.57% | 253.82 | 134.76 | -0.03% |
| 24.08 | 10.554 | -0.81% | 120.81 | 78.731 | 0.00% | 253.83 | 134.40 | -0.30% |
| 26.08 | 12.440 | -0.74% | 120.89 | 78.332 | -0.55% | 260.81 | 137.75 | 0.04% |
| 26.09 | 12.512 | -0.23% | 127.80 | 81.925 | 0.08% | 260.82 | 137.35 | -0.25% |
| 28.08 | 14.520 | 0.15% | 127.88 | 81.412 | -0.60% | 267.80 | 140.74 | 0.10% |
| 28.08 | 14.514 | 0.09% | 134.80 | 84.892 | -0.07% | 267.80 | 140.36 | -0.17% |
| 30.07 | 16.533 | 0.24% | 134.89 | 84.409 | -0.68% | | | |

[a] Standard uncertainty of temperature is $u(T)$=0.004 K, and the combined expanded uncertainty of heat capacity $U_c(C_{pm})$ with 0.95 level of confidence ($k$=2) is: $U_c(C_{pm})$=0.1 $C_{pm}$ below 10 K; $U_c(C_{pm})$=0.03 $C_{pm}$ in temperature range (10 to 40) K; $U_c(C_{pm})$=0.02 $C_{pm}$ in temperature range (40 to 300) K. Values are reported with more digits than is justified by the experimental uncertainty to avoid round-off errors in calculations based on these results. Measurements are performed in vacuum (residual pressure $p<10^{-4}$ Pa).

[b] $\delta_{rel}$ is the percentage deviation of experimental heat capacity data from the smoothed values from equations SI1 and SI2 with parameters from Table S15.

**Table S15.** Parameters of eqs SI1 and SI2 for solid phase heat capacities in $J \cdot K^{-1} \cdot mol^{-1}$.

| $a_i$ | $b_i$ | $c_i$ | $d_i$ | $T_i$ / K | $T_{i+1}$ / K | $N^a$ | $s_r^b$ |
|---|---|---|---|---|---|---|---|
| Citric Acid | | | $b$ = 0.14 | | | | |
| 6.43055E-03 | -9.84265E-02 | 1.65531E-01 | 1.00141E+01 | 0 | 6 | 14 | 1.48 |
| -3.47748E-04 | 1.73234E-02 | -3.21088E-01 | 8.85291E+00 | 6 | 21 | 16 | 0.60 |
| -1.63414E-05 | 1.67473E-03 | -3.61161E-02 | 6.76070E+00 | 21 | 55 | 18 | 0.24 |
| -7.36289E-07 | 7.91227E-06 | 2.10938E-02 | 6.82646E+00 | 55 | 113 | 25 | 0.35 |
| 1.14448E-07 | -1.20202E-04 | 1.45810E-02 | 7.93286E+00 | 113 | 350 | 104 | 0.13 |
| cis-Aconitic Acid | | | $b$ = 0.15 | | | | |
| 0 | -2.74007E-04 | -1.02531E-02 | 6.71609E+00 | 270 | 335 | 14 | 0.36 |
| $\alpha$-Ketoglutaric Acid | | | $b$ = 0.15 | | | | |
| 0 | 0 | -1.45106E-02 | 8.15627E+00 | 270 | 290 | 5 | 0.11 |
| Succinic Acid *stable* | | | $b$ = 0.15 | | | | |
| -3.64868E-05 | 5.36300E-03 | -2.43237E-01 | 1.10682E+01 | 0 | 45 | 25 | 2.33 |
| -3.11579E-06 | 4.37284E-04 | 1.77761E-02 | 7.65783E+00 | 45 | 110 | 15 | 0.17 |
| 9.30711E-08 | -1.70295E-04 | 3.51304E-02 | 9.80513E+00 | 110 | 354 | 65 | 0.24 |
| Succinic Acid *metastable* | | | $b$ = 0.16 | | | | |
| 2.75603E-03 | -5.96916E-02 | 2.03768E-01 | 1.03972E+01 | 0 | 8 | 27 | 1.16 |
| -6.18843E-05 | 6.45325E-03 | -2.22139E-01 | 9.61813E+00 | 8 | 40 | 28 | 1.05 |
| -3.28496E-06 | 5.12356E-04 | 7.60438E-04 | 7.08998E+00 | 40 | 107 | 27 | 0.48 |
| 6.49085E-08 | -1.47922E-04 | 2.51775E-02 | 8.45290E+00 | 107 | 355 | 66 | 0.18 |
| Fumaric Acid *stable* | | | $b$ = 0.16 | | | | |
| -2.17639E-03 | 2.48314E-02 | -1.41793E-01 | 9.21686E+00 | 0 | 5 | 12 | 1.17 |
| 5.00308E-04 | -7.81438E-03 | -5.67075E-02 | 8.85663E+00 | 5 | 12 | 10 | 0.85 |
| -2.18198E-05 | 2.69209E-03 | -9.25636E-02 | 8.24838E+00 | 12 | 50 | 24 | 0.22 |
| -1.53486E-06 | 2.04625E-04 | 1.75114E-02 | 7.42104E+00 | 50 | 128 | 30 | 0.26 |
| 1.79101E-07 | -1.54533E-04 | 2.14186E-02 | 9.30350E+00 | 128 | 350 | 57 | 0.14 |
| Fumaric Acid *metastable* | | | $b$ = 0.16 | | | | |
| 3.16108E-03 | -6.40476E-02 | 3.36609E-01 | 8.05306E+00 | 0 | 7 | 24 | 0.75 |
| -1.54355E-05 | 2.33499E-03 | -9.53797E-02 | 8.35523E+00 | 7 | 55 | 36 | 0.51 |
| -1.13070E-06 | 1.12278E-04 | 2.20890E-02 | 7.44978E+00 | 55 | 128 | 28 | 0.40 |
| 1.07208E-07 | -1.35345E-04 | 2.04051E-02 | 9.22074E+00 | 128 | 355 | 58 | 0.19 |
| D-Malic Acid | | | $b$ = 0.15 | | | | |
| 2.03280E-02 | -3.00570E-01 | 1.32991E+00 | 7.16850E+00 | 0 | 5 | 12 | 0.73 |
| -3.77962E-05 | 4.35019E-03 | -1.51185E-01 | 8.84482E+00 | 5 | 41 | 32 | 0.86 |
| -1.64392E-06 | 2.68204E-04 | 1.50768E-02 | 7.27657E+00 | 41 | 128 | 32 | 0.38 |
| 9.73316E-08 | -1.60858E-04 | 2.44158E-02 | 9.53576E+00 | 128 | 335 | 56 | 0.17 |
| Oxaloacetic Acid | | | $b$ = 0.16 | | | | |
| 9.63794E-03 | -2.00621E-01 | 1.31820E+00 | 5.18556E+00 | 0 | 7 | 16 | 0.80 |
| -1.06814E-05 | 1.77549E-03 | -7.37193E-02 | 7.88834E+00 | 7 | 60 | 34 | 0.47 |
| -1.30779E-06 | 7.71501E-05 | 2.44707E-02 | 7.37836E+00 | 60 | 122 | 24 | 0.51 |
| 1.74226E-07 | -1.66098E-04 | 1.89559E-02 | 8.88042E+00 | 122 | 340 | 57 | 0.28 |

[a] $N$ stands for number of experimental data points in given temperature interval used for correlation.

[b] $s_r = 100\left\{\sum_{i=1}^{n}\left[\left(C_{pm}^{exp} - C_{pm}^{calc}\right)/C_{pm}^{calc}\right]_i^2 \Big/ (n-m)\right\}^{1/2}$, where $n$ is the number of fitted data points, and $m$ is the number of independent adjustable parameters for the given interval.

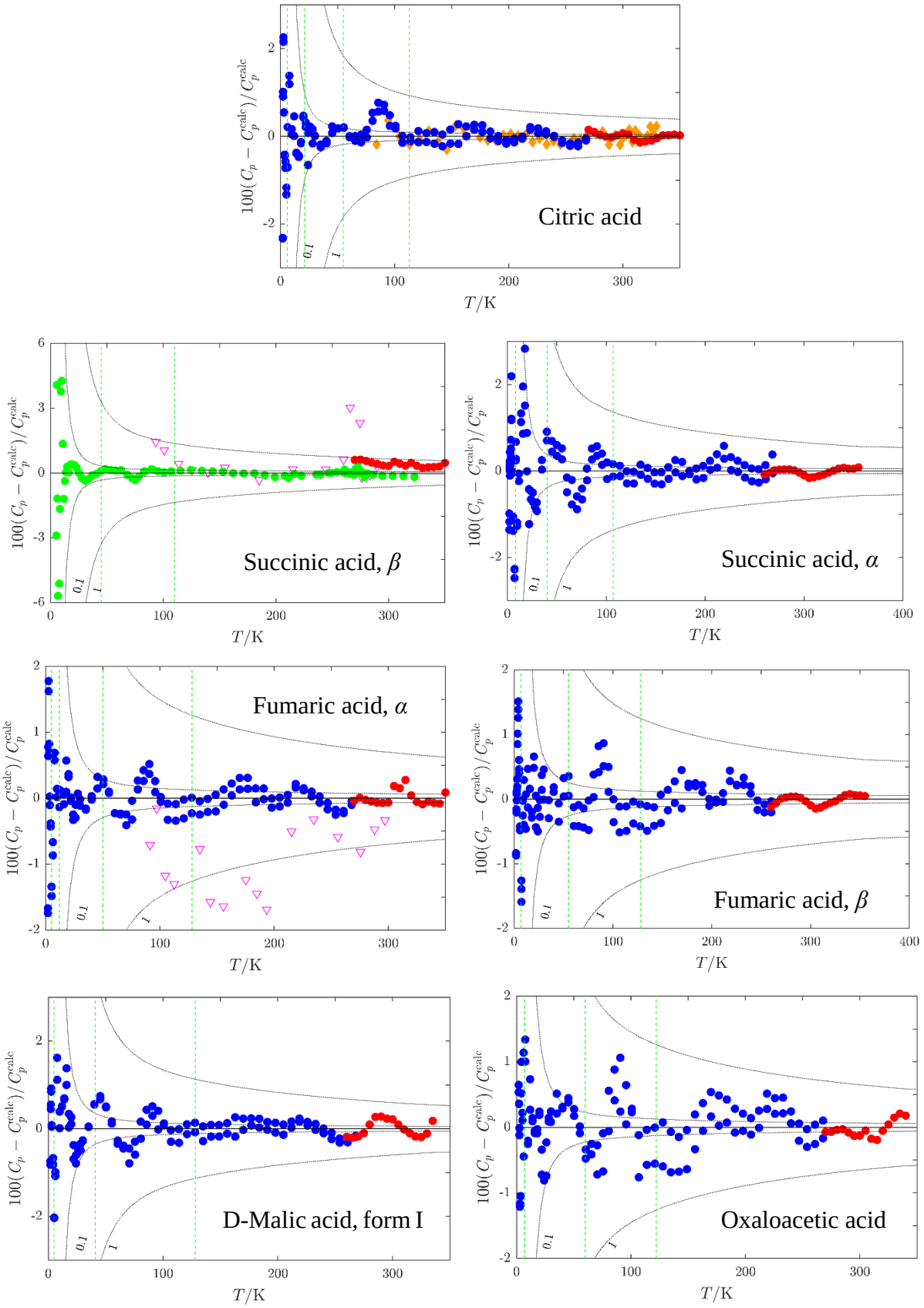


**Figure S23.** Relative deviations $100\left(C_{pm}^{exp} - C_{pm}^{fit}\right)/C_{pm}^{fit}$ of individual experimental heat capacities $C_{pm}^{exp}$ from values $C_{pm}^{fit}$ calculated by means of eqs. SI1 and SI2 with parameters from Table S15. ●, This work (relaxation calorimetry); ●, This work (Tian-Calvet calorimetry); ◆, de Kruif et al.[45]; ▽, Parks and Huffman[42]; ●, Vanderzee and Westrum.[69] Green vertical lines mark knot temperatures $T_i$, black dotted lines are absolute deviations in J $K^{-1}$ $mol^{-1}$.

## SI6.4 Computational interpretation of the heat capacity trends

Correlations of selected phonon-based descriptors calculated for individual crystals discussed in section 4.5 are depicted in Figure S24 and the complete calculated phonon density of states are visualized in Figure S25.

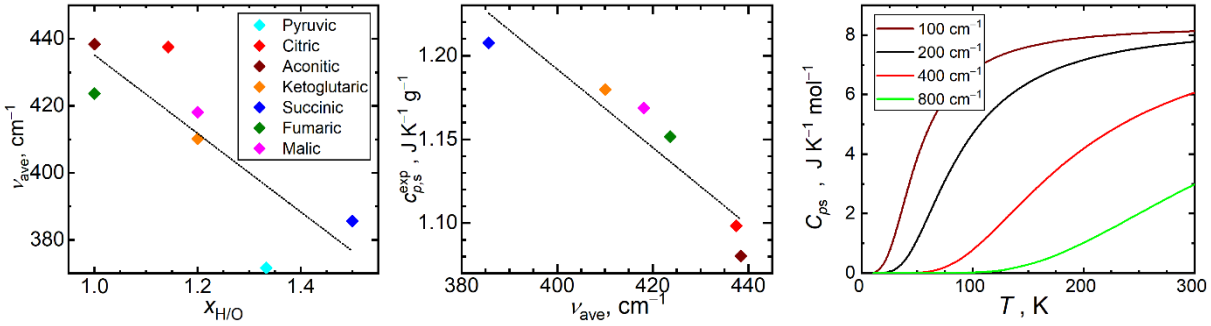


**Figure S24.** Left – correlation of the stoichiometric ratio of H and O atoms with the calculated mean vibrational frequency $\nu_{ave}$ of the crystals; in the region 0-1000 cm$^{-1}$; center – correlation of $\nu_{ave}$ with the experimental specific heat capacity of the crystals; right – magnitude of model contributions from individual vibration modes to the molar heat capacity of crystals.

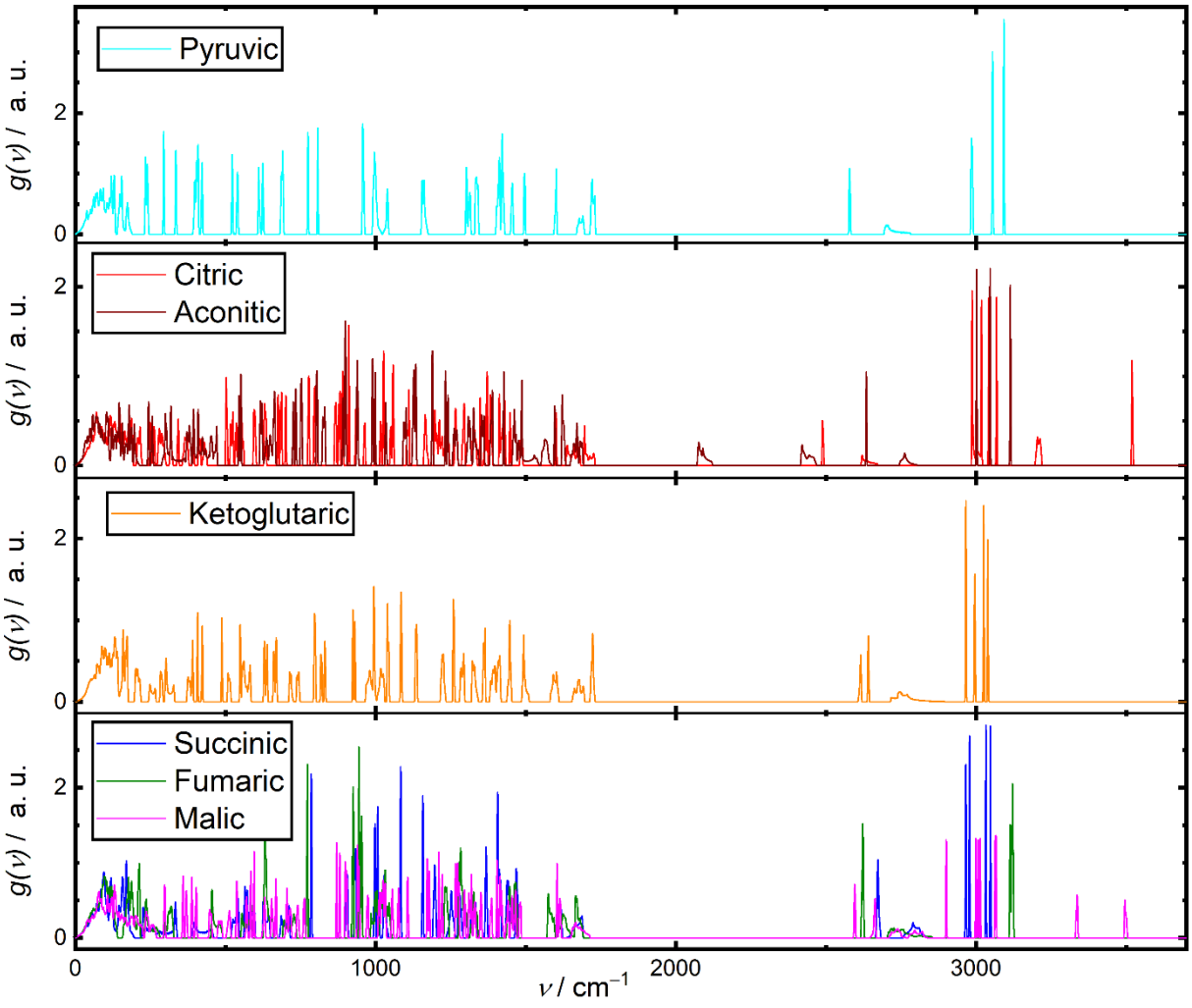


**Figure S25.** Densities of phonon states calculated at the PBE-D3/PAW level of theory for the unit-cell volumes corresponding to the minima of the electronic energy vs. volume curves.

## SI6.5 Controlled extrapolation of heat capacities down from the ambient region

We propose the following three-step procedure to extrapolate experimental heat capacities of molecular crystals from the ambient region to low temperatures using the theoretical data using: i) to evaluate the ratio $C_p^{\mathrm{calc}}/C_p^{\mathrm{exp}}$ using experimental data in the (nearly-)ambient region; ii) to extrapolate this ratio towards 0 K, optionally constraining its value equal to unity at 0 K; iii) scaling the quasi-harmonic $C_p^{\mathrm{calc}}$ by that extrapolated $C_p^{\mathrm{calc}}/C_p^{\mathrm{exp}}$ ratio. We tested either constant, linear, quadratic, and cubic extrapolation of the $C_p^{\mathrm{calc}}/C_p^{\mathrm{exp}}$ ratio (Figure S26), out of which the linear proved as the most reliable (Figure S27). The resulting theoretical heat capacities scaled to experimental values are listed in Table S16.

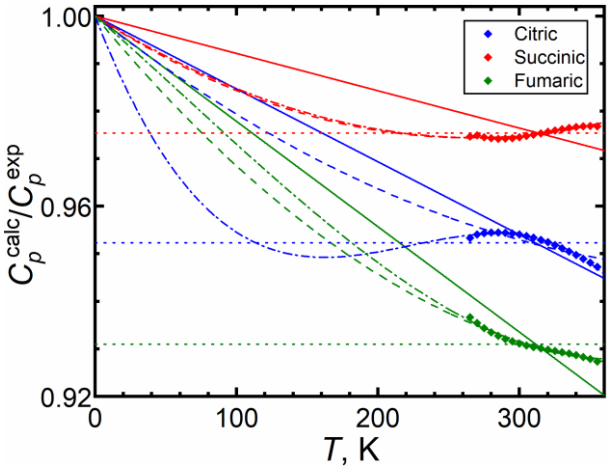


**Figure S26.** Ratio of quasi-harmonic PBE-D3/PAW and experimental isobaric heat capacities and comparison of various extrapolative schemes used to scale the calculated data at lower temperatures: dotted – average; solid – linear; dashed – quadratic; dash-dotted – cubic.

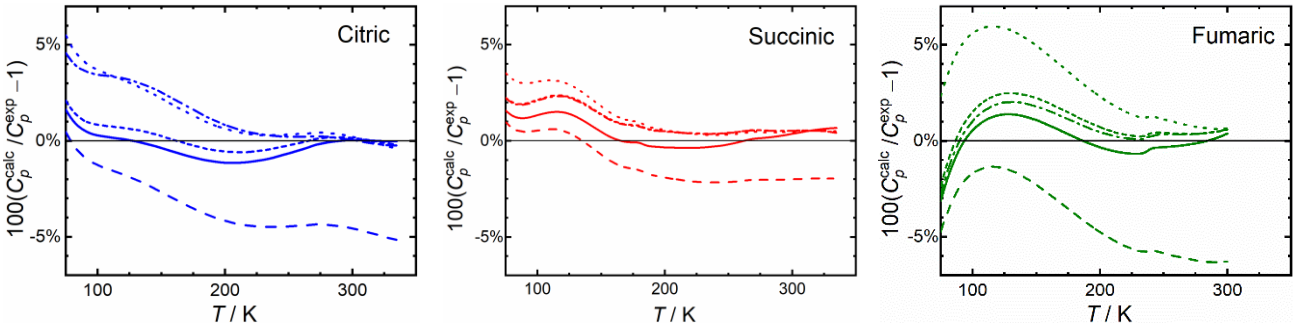


**Figure S27.** Percentage deviations of quasi-harmonic PBE-D3/PAW isobaric heat capacities from the experiment. Comparison of the performance of various extrapolative scaling approaches: dotted – average; solid – linear; dashed – quadratic; dash-dotted – cubic extrapolation of the $C_p^{\mathrm{calc}}/C_p^{\mathrm{exp}}$ ratio.

**Table S16**: Isobaric heat capacities[a] of crystalline carboxylic acids $C_{p,m}$ (J K$^{-1}$ mol$^{-1}$) obtained according to our controlled extrapolation combining experimental data in the ambient region and results of quasi-harmonic PBE-D3/PAW calculations as explained in section SI6.4.

| Acid | Pyruvic[b] | Citric | *cis*-Aconitic | *α*-Keto-glutaric | Succinic | Fumaric | Malic |
|---|---|---|---|---|---|---|---|
| $T$ / K | | | | | $C_{p,m}^{calc}$ | | |
| 15 | 4.93 | 5.78 | 7.45 | 4.29 | 4.06 | 3.96 | 4.32 |
| 20 | 9.71 | 12.84 | 14.26 | 10.46 | 9.51 | 8.99 | 9.63 |
| 25 | 14.15 | 19.86 | 20.48 | 16.76 | 14.95 | 14.01 | 14.89 |
| 30 | 18.35 | 26.59 | 26.41 | 22.77 | 20.10 | 18.79 | 19.93 |
| 35 | 22.32 | 33.04 | 32.04 | 28.50 | 24.96 | 23.35 | 24.75 |
| 40 | 26.07 | 39.24 | 37.41 | 33.97 | 29.57 | 27.70 | 29.36 |
| 45 | 29.62 | 45.19 | 42.53 | 39.19 | 33.93 | 31.85 | 33.78 |
| 50 | 32.97 | 50.91 | 47.41 | 44.17 | 38.05 | 35.81 | 38.02 |
| 60 | 39.15 | 61.71 | 56.53 | 53.48 | 45.67 | 43.18 | 45.98 |
| 70 | 44.70 | 71.72 | 64.90 | 62.00 | 52.51 | 49.90 | 53.33 |
| 80 | 49.69 | 81.03 | 72.63 | 69.81 | 58.70 | 56.04 | 60.14 |
| 90 | 54.20 | 89.73 | 79.82 | 77.01 | 64.31 | 61.65 | 66.49 |
| 100 | 58.30 | 97.91 | 86.57 | 83.68 | 69.46 | 66.81 | 72.44 |
| 110 | 62.06 | 105.63 | 92.96 | 89.89 | 74.22 | 71.59 | 78.07 |
| 120 | 65.53 | 112.97 | 99.09 | 95.73 | 78.66 | 76.03 | 83.41 |
| 130 | 68.77 | 120.00 | 105.01 | 101.26 | 82.86 | 80.19 | 88.55 |
| 140 | 71.82 | 126.76 | 110.79 | 106.54 | 86.89 | 84.13 | 93.51 |
| 150 | 74.73 | 133.32 | 116.49 | 111.64 | 90.79 | 87.89 | 98.35 |
| 160 | 77.52 | 139.72 | 122.14 | 116.59 | 94.63 | 91.52 | 103.11 |
| 170 | 80.23 | 146.00 | 127.79 | 121.45 | 98.45 | 95.07 | 107.82 |
| 180 | 82.89 | 152.22 | 133.45 | 126.26 | 102.29 | 98.57 | 112.52 |
| 190 | 85.50 | 158.38 | 139.15 | 131.06 | 106.17 | 102.05 | 117.23 |
| 200 | 88.09 | 164.54 | 144.89 | 135.86 | 110.13 | 105.55 | 121.96 |
| 210 | 90.65 | 170.69 | 150.66 | 140.71 | 114.19 | 109.10 | 126.75 |
| 220 | 93.20 | 176.86 | 156.46 | 145.60 | 118.34 | 112.72 | 131.59 |
| 230 | 95.72 | 183.06 | 162.25 | 150.56 | 122.61 | 116.43 | 136.48 |
| 240 | 98.20 | 189.30 | 167.95 | 155.85 | 126.99 | 120.53 | 141.43 |
| 250 | 100.62 | 195.56 | 173.81 | 160.85 | 131.46 | 124.31 | 146.44 |
| 260 | 102.97 | 201.84 | 179.65 | 165.80 | 136.02 | 128.08 | 151.48 |

[a] Calculated $C_{p,m}$ values scaled using the linear extrapolative scheme to match the experimental data, expected uncertainty below 2 % above 100 K, and below 5 J K$^{-1}$ mol$^{-1}$ otherwise.
[b] Calculated $C_{p,m}$ unscaled due to the lack of reliable experimental data.

## SI6.6 Modelling the static disorder and of carboxylic protons and polymorphism

The extent of the static disorder relevant to both polymorphs of succinic and fumaric acid was assessed using the electronic energies of the supercells depicted in Figure S28, which were extracted from single-point PBE-D3/PAW calculations. These supercells were built from original unit cells and unit cells perturbed at exactly one carboxyl site. These unit cells were previously optimized in periodic boundary conditions in both cases.

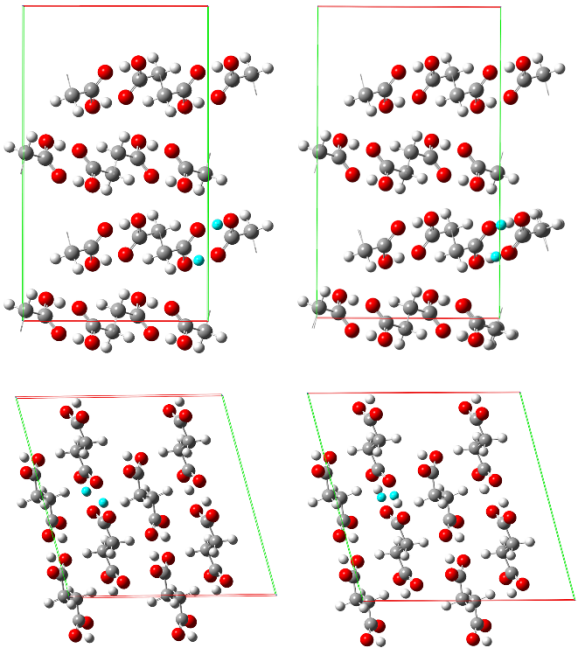

**Figure S28.** Geometries of 2x2x2 supercells of β succinic acid (upper row) and α succinic acid (lower row), with hydrogen atoms within a selected carboxyl dimer marked. Left column depicts the unperturbed crystal structures, whereas the right column illustrates the structures after interchange of the hydrogen atoms within those selected carboxyl dimers.

The multi-level approach QM/QM adopted in the fragment-based scheme for calculations of the cohesive energies can be exploited to compare cohesive energy and its contributions computed by various methods. Table S17 lists such data obtained in this work.

**Table S17**: Differences of cohesive energies or their short-range contributions related to phase transitions. All data given in kJ mol$^{-1}$.

| | Succinic (β→α) | Fumaric (α→β) | Malic (I→II) |
|---|---|---|---|
| Full cohesive energies | | | |
| PBE-D3/PAW | −0.69 | +3.30 | −3.31 |
| B3LYP-D3/pob-TZVP-rev2 | +1.22 | +4.93 | −5.96 |
| DW-CCSD(T)-F12/aug-cc-pVDZ&\|B3LYP-D3/pob-TZVP-rev2 | +0.98 | +2.12 | −2.72 |
| One+two-body contributions | | | |
| B3LYP-D3/pob-TZVP-rev2 | +2.28 | +7.53 | +1.39 |
| DW-CCSD(T)-F12/aug-cc-pVDZ | +2.05 | +4.72 | +4.63 |

## Section SI7 References to the Supporting Information


1. J. C. Lashley, M. F. Hundley, A. Migliori, J. L. Sarrao, P. G. Pagliuso, T. W. Darling, M. Jaime, J. C. Cooley, W. L. Hults, L. Morales, D. J. Thoma, J. L. Smith, J. Boerio-Goates, B. F. Woodfield, G. R. Stewart, R. A. Fisher and N. E. Phillips, *Cryogenics*, 2003, **43**, 369-378.
2. T. Mahnel, V. Pokorný, M. Fulem, D. Sedmidubský and K. Růžička, *J. Chem. Thermodyn.*, 2020, **142**, 105964.
3. D. G. Archer, *J. Phys. Chem. Ref. Data*, 1992, **21**, 1-21.
4. K. Harata, N. Sakabe and J. Tanaka, *Acta Crystallogr. B*, 1977, **33**, 210-212.
5. A. Rammohan and J. A. Kaduk, *Acta Crystallogr. Sect. B*, 2018, **74**, 239-252.
6. T. Lis and J. Matuszewski, *Acta Crystallogr. C*, 1984, **40**, 2016-2019.
7. C. Brown, *Acta Crystallogr.*, 1966, **21**, 1-5.
8. J.-L. Leviel, G. Auvert and J.-M. Savariault, *Acta Crystallogr. B*, 1981, **37**, 2185-2189.
9. N. N. Petropavlov and S. B. Yarantsev, *Crystallogr. Rep. Russ,*, 1983, **28**, 1132.
10. I. M. Dodd, S. J. Maginn, M. M. Harding and R. J. Davey, *CSD Communication*, 1998, CCDC 1263474.
11. J. S. Broadley, D. W. J. Cruickshank, J. D. Morrison, J. M. Robertson and H. M. M. Shearer, *Proc. R. Soc. A*, 1959, **251**, 441-457.
12. V. R. Thalladi, M. Nüsse and R. Boese, *J. Am. Chem. Soc.*, 2000, **122**, 9227-9236.
13. S. Bhattacharya, V. G. Saraswatula and B. K. Saha, *Cryst. Growth Des.*, 2013, **13**, 3651-3656.
14. P. van der Sluis and J. Kroon, *Acta Crystallogr. C*, 1989, **45**, 1406-1408.
15. A. Boultif and D. Louer, *J. Appl. Crystallogr.*, 2004, **37**, 724-731.
16. R. Oishi-Tomiyasu, *J. Appl. Crystallogr.*, 2014, **47**, 593-598.
17. V. Petříček, M. Dušek and L. Palatinus, *Z. Kristallogr. Cryst. Mater.*, 2014, **229**, 345-352.
18. L. Palatinus and G. Chapuis, *J. Appl. Crystallogr.*, 2007, **40**, 786-790.
19. J. Rohlíček and M. Hušák, *J. Appl. Crystallogr.*, 2007, **40**, 600-601.
20. D. Heger, A. J. Eugene, S. R. Parkin and M. I. Guzman, *Acta Crystallogr. E*, 2019, **75**, 858-862.
21. A. V. Churakov, *Experimental Crystal Structure Determination*, 2007, CCDC 635772.
22. N. Nagel, U. Endruschat and H. Bock, *Acta Crystallogr. C*, 1996, **52**, 2912-2915.
23. R. Srinivasa Gopalan, P. Kumaradhas, G. U. Kulkarni and C. N. R. Rao, *J. Mol. Struct.*, 2000, **521**, 97-106.
24. M. K. Mishra, U. Ramamurty and G. R. Desiraju, *Chem. Asian J.*, 2015, **10**, 2176-2181.
25. P. Lucaioli, E. Nauha, I. Gimondi, L. S. Price, R. Guo, L. Iuzzolino, I. Singh, M. Salvalaglio, S. L. Price and N. Blagden, *CrystEngComm*, 2018, **20**, 3971-3977.
26. G. D. Rieck, *Recl. Trav. Chim. Pays-Bas*, 1944, **63**, 170-180.
27. I. M. Dodd, S. J. Maginn, M. M. Harding and R. J. Davey, *CSD Communication*, 1998, CCDC 1263475.
28. A. L. Bednowitz and B. Post, *Acta Crystallogr.*, 1966, **21**, 566-571.
29. J. Yang, C. T. Hu, A. G. Shtukenberg, Q. Yin and B. Kahr, *CrystEngComm*, 2018, **20**, 1383-1389.
30. P. van der Sluis and J. Kroon, *Acta Crystallogr. Sect. C*, 1985, **41**, 956-959.
31. D. Wyrzykowski, E. Hebanowska, G. Nowak-Wiczk, M. Makowski and L. Chmurzyński, *J. Therm. Anal. Calorim.*, 2011, **104**, 731-735.
32. R. C. Wilhoit and D. Shiao, *J. Chem. Eng. Data*, 1964, **9**, 595-599.
33. H. Groen and K. J. Roberts, *J. Phys. Chem. B*, 2001, **105**, 10723-10730.
34. C. H. Sorum and E. A. Durand, *J. Am. Chem. Soc.*, 1952, **74**, 1071-1073.
35. G. G. Lobbia, G. Berchiesi and M. A. Berchiesi, *J. Therm. Anal.*, 1976, **10**, 205-209.
36. M. V. Roux, M. Temprado and J. S. Chickos, *J. Chem. Thermodyn.*, 2005, **37**, 941-953.
37. M. Leclercq, A. Collet and J. Jacques, *Tetrahedron*, 1976, **32**, 821-828.

38. R. C. Wilhoit and I. Lei, *J. Chem. Eng. Data*, 1965, **10**, 166-168.
39. I. Contineanu, L. Chivu and Ş. Perişanu, *Revista de Chimie*, 2005, **56**, 719-721.
40. H. J. H. Fenton and W. A. R. Wilks, *Journal of the Chemical Society, Transactions*, 1912, **101**, 1570-1582.
41. Q. Yu, L. Dang, S. Black and H. Wei, *J. Cryst. Growth*, 2012, **340**, 209-215.
42. G. S. Parks and H. M. Huffman, *J. Am. Chem. Soc.*, 1930, **52**, 4381-4391.
43. R. C. Wilhoit, J. Chao and K. R. Hall, *J. Phys. Chem. Ref. Data*, 1985, **14**, 1-175.
44. G. Bruni, M. Maietta, L. Maggi, M. Bini, D. Capsoni, S. Ferrari, M. Boiocchi, V. Berbenni, C. Milanese and A. Marini, *CrystEngComm*, 2012, **14**, 6035-6044.
45. C. G. de Kruif, J. C. van Miltenburg, A. J. J. Sprenkels, G. Stevens, W. de Graaf and H. G. M. de Wit, *Thermochim. Acta*, 1982, **58**, 341-354.
46. W. Acree and J. S. Chickos, *J. Phys. Chem. Ref. Data*, 2016, **45**, 033101.
47. A. Forster, J. Hempenstall, I. Tucker and T. Rades, *Int. J. Pharm.*, 2001, **226**, 147-161.
48. M. Tomassetti, A. Catalani, V. Rossi and S. Vecchio, *J. Pharm. Biomed. Anal.*, 2005, **37**, 949-955.
49. K. Klímová and J. Leitner, *Thermochim. Acta*, 2012, **550**, 59-64.
50. A. M. Booth, M. H. Barley, D. O. Topping, G. McFiggans, A. Garforth and C. J. Percival, *Atmos. Chem. Phys.*, 2010, **10**, 4879-4892.
51. K. A. Park, H. J. Lee and I. K. Hong, *Journal of Industrial and Engineering Chemistry*, 2010, **16**, 490-495.
52. V. Meltzer and E. Pincu, *Open Chemistry*, 2012, **10**, 1584-1589.
53. S. Shantikumar, G. Sreekanth, K. V. SurendraNath, S. JaferValli and N. Satheeshkumar, *J. Therm. Anal. Calorim.*, 2014, **115**, 2423-2428.
54. J. M. Weiss and C. R. Downs, *J. Am. Chem. Soc.*, 1923, **45**, 1003-1008.
55. C. Marques, A. R. Sotiles, F. O. Farias, G. Oliveira, M. L. Mitterer-Daltoé and M. L. Masson, *Arabian Journal of Chemistry*, 2020, **13**, 9118-9129.
56. R. Ceolin, H. Szwarc and F. Lepage, *Thermochim. Acta*, 1990, **158**, 347-352.
57. Q. Zhang, Y. Yang, L. Cheng, C. Cao, Z. Ding, C. Wang, W. Yang, Y. Hu and Y. Li, *J. Chem. Thermodyn.*, 2015, **85**, 148-154.
58. Z. Gao, Y. Li and X. Wang, *J. Mol. Liq.*, 2021, **325**, 115113.
59. C. Heidelberger, *Biochem. Prep.*, 1953, **3**, 59-61.
60. F. Dupré la Tour, *Ann. Phys.*, 1932, **18**, 199-283.
61. J. D. Morrison and J. M. Robertson, *J. Chem. Soc.*, 1949, **0**, 980-986.
62. S.-W. S. Wong and E. F. Westrum, *J. Am. Chem. Soc.*, 1971, **93**, 5317-5321.
63. A. Cingolani and G. Berchiesi, *J. Therm. Anal.*, 1974, **6**, 87-90.
64. S. C. Khetarpal, K. Lal and H. L. Bhatnagar, *Indian J. Chem., Sect. A*, 1980, **19A**, 634-640.
65. M. A. V. Ribeiro da Silva, M. J. S. Monte and J. R. Ribeiro, *J. Chem. Thermodyn.*, 2001, **33**, 23-31.
66. Y. Li, Y. Wang, Z. Ning, J. Cui, Q. Wu and X. Wang, *J. Chem. Eng. Data*, 2014, **59**, 4062-4069.
67. K. J. Paluch, T. McCabe, H. Müller-Bunz, O. I. Corrigan, A. M. Healy and L. Tajber, *Mol. Pharmaceut.*, 2013, **10**, 3640-3654.
68. W. Yang, X. Jiang, Y. Hu, Y. Shi, H. Sun and Y. Li, *J. Solution Chem.*, 2013, **42**, 1591-1601.
69. C. E. Vanderzee and E. F. Westrum, *J. Chem. Thermodyn.*, 1970, **2**, 681-687.